NASA TECHNICAL NOTE

NASA TN D-8085 $c.1$

NASA TN D-8085
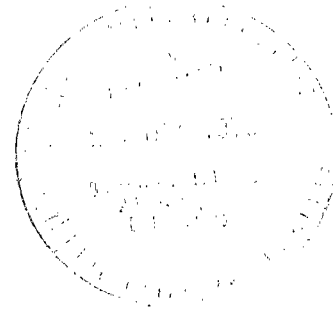
FLUTTER ANALYSIS OF TWO PARALLEL ELASTICALLY COUPLED FLAT PLATES

Charles P. Shore

Langley Research Center
Hampton, Va. 23665

NATIONAL AERONAUTICS AND SPACE ADMINISTRATION • WASHINGTON, D. C. • DECEMBER 1975

1. Report No. NASA TN D-8085	2. Government Accession No.	3. Recipient's Catalog No.
4. Title and Subtitle FLUTTER ANALYSIS OF TWO PARALLEL ELASTICALLY COUPLED FLAT PLATES		5. Report Date December 1975
		6. Performing Organization Code
7. Author(s) Charles P. Shore		8. Performing Organization Report No. L-10443
		10. Work Unit No. 505-02-12-01
9. Performing Organization Name and Address NASA Langley Research Center Hampton, Va. 23665		11. Contract or Grant No.
		13. Type of Report and Period Covered Technical Note
12. Sponsoring Agency Name and Address National Aeronautics and Space Administration Washington, D.C. 20546		14. Sponsoring Agency Code

15. Supplementary Notes

16. Abstract

　　Flutter of two parallel elastically coupled flat plates is investigated analytically. A closed-form solution including both aerodynamic and structural damping is presented for flutter of flat orthotropic plates coupled by an elastic medium. Both plates are simply supported along the side edges but are supported by deflectional, rotational, and torsional springs of arbitrary stiffness at the leading and trailing edges. Two-dimensional quasi-steady aerodynamics is utilized in the solution. Since the large number of variables present in the problem precludes extensive parametric studies, results are presented to indicate the basic flutter characteristics of coupled two-plate systems and to assess the validity of previously published modal solutions for similar problems.

17. Key Words (Suggested by Author(s)) Panel flutter Buckling Damping Elastic coupling Vibration	18. Distribution Statement Unclassified — Unlimited Subject Category 39		
19. Security Classif. (of this report) Unclassified	20. Security Classif. (of this page) Unclassified	21. No. of Pages 40	22. Price* $3.75

FLUTTER ANALYSIS OF TWO PARALLEL ELASTICALLY
COUPLED FLAT PLATES

Charles P. Shore
Langley Research Center

SUMMARY

Flutter of two parallel elastically coupled flat plates is investigated analytically. A closed-form solution including both aerodynamic and structural damping is presented for flutter of flat orthotropic plates coupled by an elastic medium. Both plates are simply supported along the side edges but are supported by deflectional, rotational, and torsional springs of arbitrary stiffness at the leading and trailing edges. Two-dimensional quasi-steady aerodynamics is utilized in the solution. Since the large number of variables present in the problem precludes extensive parametric studies, results are presented to indicate the basic flutter characteristics of coupled two-plate systems and to assess the validity of previously published modal solutions for similar problems.

INTRODUCTION

Flutter of two simply supported parallel isotropic plates connected by an elastic medium has been investigated previously in connection with micrometeroid bumpers which are attached to a primary structural skin by a light soft filler material. Although intended primarily as a protective device in space, such configurations must withstand severe aerodynamic loads during launch. In reference 1 a two-mode Galerkin solution to the coupled fourth-order differential equations describing motion of the two plates was obtained. The simple Ackeret expression for the lateral loading due to air pressure was used in the analysis. In reference 2 a two-mode flutter solution which used piston theory aerodynamics to incorporate aerodynamic damping effects was obtained for the coupled-plate problem. In addition a semiexact procedure and a finite-difference formulation were outlined; however, the only results presented were from the two-mode solution. Results presented in references 1 and 2 indicate that the elastic coupling medium can have significant effects on the flutter response of the two-plate system. In fact, depending on the magnitude of inplane loads acting on the plates and the spring stiffness of the elastic coupling medium, the two-plate system can become unstable at much lower dynamic pressures than either of the two plates alone.

More recently several thermal protection systems which employ exposed surfaces coupled to primary load carrying structures by flexible insulation and/or strain-isolator

systems have been proposed for space shuttle and hypersonic cruise vehicles. The flutter characteristics of reusable surface insulation (RSI) panels coupled to a primary structure by a flexible strain isolator have been studied in reference 3. The analysis utilizes plate modes for the simply supported primary structure and free-free beam modes for the RSI panels. Dynamic response of the coupled system was obtained by application of the Rayleigh-Ritz technique. Results presented in reference 3 indicate that the presence of the RSI panels has a highly stabilizing effect on the flutter response of the primary structure. The main cause of the increased flutter stability of the primary structure was attributed to the segmented mode shapes of the RSI panels which govern the interaction of the aerodynamic forces and the deflections of the primary structure. Finally, the typical severely destabilizing influence of midplane compressive loads on single isotropic panels was not always observed for the coupled system, and the buckling value of the midplane loading for the primary structure was found to be increased significantly by the RSI/strain-isolator system.

In many instances the exposed surfaces of typical thermal protection systems consist of highly orthotropic panels with arbitrary flexible supports at the boundaries. (See ref. 4.) Thus, the present report extends the previous solutions to a more general configuration consisting of two parallel orthotropic plates connected by an elastic medium and supported at the leading and trailing edges on springs of arbitrary stiffness. Piston theory aerodynamics is employed to obtain the lateral loading due to air pressure over the exposed plate, and taking the side edges of the plates to be simply supported allows a closed-form solution (i.e., nonmodal) to the governing partial differential equations. Results from the analysis are compared with results from references 1 to 3, and a general flutter boundary for two identical simply supported coupled plates is presented for a single value of the elastic spring stiffness of the connecting medium. Specific examples are also presented to indicate the applicability of the solution and to indicate some effects of structural damping and inplane loading on the flutter of elastically coupled parallel plates. Additionally, the influence on flutter of single plates with unequal support springs at the leading and trailing edges is briefly discussed.

SYMBOLS

Dimensional quantities are presented both in the International System of Units (SI) and in the U.S. Customary Units. Measurements were made in U.S. Customary Units.

A_i deflection shape coefficients

$\overline{A}$ parameter defined by equation (16)

a plate length

$\overline{B}$ parameter defined by equation (17)

b   plate width

c   free-stream speed of sound

D_x plate bending stiffness in x-direction

D_y plate bending stiffness in y-direction

D_{xy} plate twisting stiffness

D_1,D_2 plate stiffness coefficients defined by equation (7)

E   Young's modulus

G_d,G_t,G_r complex deflectional, torsional, and rotational support spring coeffi-
             cients defined by equation (11)

G_x,G_{xy},G_y complex coefficients defined by equation (8)

g_a aerodynamic damping coefficient, $\rho c / \gamma_U \omega_{r,U}$

g_d,g_t,g_r deflectional, torsional, and rotational support spring structural damping
             coefficients

g_k elastic coupling-medium structural damping coefficient

g_x,g_{xy},g_y plate structural damping coefficients

I   moment of inertia

i   imaginary unit, $\sqrt{-1}$

K   complex spring stiffness of elastic coupling medium

k   spring stiffness of elastic coupling medium in compression

k_d,k_t,k_r deflectional, torsional, and rotational spring stiffnesses

3

$l(x,y,t)$ aerodynamic loading term

M Mach number

m number of half-waves in streamwise direction

N_x inplane loading in x-direction, positive in compression

N_y inplane loading in y-direction, positive in compression

n number of tiles

P_i roots to equation (22)

q free-stream dynamic pressure

R_x nondimensional inplane loading parameter in x-direction, $N_x b^2 / \pi^2 D_1$

$R_{x,cr}$ buckling load with no airflow

R_y nondimensional inplane loading parameter in y-direction, $N_y b^2 / \pi^2 D_1$

S coupling-medium spring parameter defined by equations (18)

t time

V free-stream velocity

w lateral deflection

X deflection shape in x-direction

x,y,z Cartesian coordinates

α_j coefficients defined by equation (A5)

β compressibility factor, $\sqrt{M^2 - 1}$

γ plate mass per unit area

ζ complex frequency coefficient, $\phi + i\omega$

λ dynamic-pressure parameter, $2qa^3 / \beta D_{1,U}$

μ_x, μ_y Poisson's ratio in x-direction and y-direction, respectively

ρ free-stream air density

ϕ real part of complex frequency exponential coefficient

$[\Omega]$ boundary condition matrix

ω circular frequency

ω_r reference frequency, see equations (18)

Subscripts:

L   lower plate

le leading edge

max   maximum

te   trailing edge

U   upper plate

Two terms, one above the other, within braces $\{ \}$ occur in the equations of this report. This notation means that two equations may be obtained by substituting first the upper and then the lower term. For example, equation (4b)

$$\frac{D_{x,U}}{1 - \mu_{x,U}\mu_{y,U}} \left(\frac{\partial^2 w_U}{\partial x^2} + \mu_{y,U} \frac{\partial^2 w_U}{\partial y^2} \right) \left\{ \begin{matrix} -k_{r,le,U} \\ +k_{r,te,U} \end{matrix} \right\} \frac{\partial w_U}{\partial x} = 0 \quad \text{at} \quad x = \left\{ \begin{matrix} 0 \\ a \end{matrix} \right\}$$

means that

$$\frac{D_{x,U}}{1 - \mu_{x,U}\mu_{y,U}} \left(\frac{\partial^2 w_U}{\partial x^2} + \mu_{y,U} \frac{\partial^2 w_U}{\partial y^2} \right) - k_{r,le,U} \frac{\partial w_U}{\partial x} = 0 \quad \text{at} \quad x = 0$$

5

and

$$\frac{D_{x,U}}{1 - \mu_{x,U}\mu_{y,U}}\left(\frac{\partial^2 w_U}{\partial x^2} + \mu_{y,U}\frac{\partial^2 w_U}{\partial y^2}\right) + k_{r,te,U}\frac{\partial w_U}{\partial x} = 0 \quad \text{at} \quad x = a$$

ANALYSIS

The configuration to be analyzed is shown in figure 1 and consists of an upper ortho-
tropic plate exposed to the airflow coupled, by a linearly elastic medium, to a lower ortho-
tropic plate. The coupling medium behaves like a Winkler foundation in that an applied
force causes deflection only at the point of application of the force. Both plates are sim-
ply supported along the side edges but are supported by deflectional, rotational, and tor-
sional springs of arbitrary stiffness at the leading and trailing edges. Each plate may
also have different material properties and inplane loadings.

Differential Equations and Boundary Conditions

The appropriate small-deflection equilibrium equations for the two orthotropic
plates in the presence of inplane tensile or compressive loads may be written in the fol-
lowing form (ref. 1):

Upper plate

$$\frac{D_{x,U}}{1 - \mu_{x,U}\mu_{y,U}}\frac{\partial^4 w_U}{\partial x^4} + 2\left(D_{xy,U} + \frac{\mu_{y,U}D_{x,U}}{1 - \mu_{x,U}\mu_{y,U}}\right)\frac{\partial^4 w_U}{\partial x^2 \partial y^2} + \frac{D_{y,U}}{1 - \mu_{x,U}\mu_{y,U}}\frac{\partial^4 w_U}{\partial y^4}$$

$$+ N_{x,U}\frac{\partial^2 w_U}{\partial x^2} + N_{y,U}\frac{\partial^2 w_U}{\partial y^2} + \gamma_U\frac{\partial^2 w_U}{\partial t^2} + k\left(w_U - w_L\right) = l(x,y,t) \tag{1}$$

Lower plate

$$\frac{D_{x,L}}{1 - \mu_{x,L}\mu_{y,L}}\frac{\partial^4 w_L}{\partial x^4} + 2\left(D_{xy,L} + \frac{\mu_{y,L}D_{x,L}}{1 - \mu_{x,L}\mu_{y,L}}\right)\frac{\partial^4 w_L}{\partial x^2 \partial y^2} + \frac{D_{y,L}}{1 - \mu_{x,L}\mu_{y,L}}\frac{\partial^4 w_L}{\partial y^4}$$

$$+ N_{x,L}\frac{\partial^2 w_L}{\partial x^2} + N_{y,L}\frac{\partial^2 w_L}{\partial y^2} + \gamma_L\frac{\partial^2 w_L}{\partial t^2} + k\left(w_L - w_U\right) = 0 \tag{2}$$

6

The subscripts U and L refer to the upper and lower plates, respectively; for each plate the bending stiffnesses in the x- and y-directions are denoted by D_x and D_y, respectively; D_{xy} denotes the plate twisting stiffness, γ is the plate mass per unit area, and k denotes the spring stiffness of the elastic coupling medium in compression. The lateral loading induced by supersonic flow over the upper plate is assumed to be given by two-dimensional quasi-steady aerodynamic theory, so that

$$\ell(x,y,t) = -\frac{2q}{\beta}\frac{\partial w_U}{\partial x} - \rho c \frac{\partial w_U}{\partial t} \tag{3}$$

where $q = \frac{1}{2}\rho V^2$ is the free-stream dynamic pressure and $\beta = \sqrt{M^2 - 1}$ is the compressibility factor. The first term on the right side of equation (3) corresponds to a static loading and the second term is an aerodynamic damping term. References 5 and 6 have shown that for M > 1.6 and a/b from 0 to 10, use of two-dimensional aerodynamic theory yields flutter results in good agreement with those predicted by more exact aerodynamic theory.

According to reference 7 the boundary conditions may be written as follows:

Upper plate

$$w_U(x,y,t) = \frac{\partial^2 w_U(x,y,t)}{\partial y^2} = 0 \qquad \text{at} \qquad y = 0 \text{ and } b \tag{4a}$$

$$\frac{D_{x,U}}{1 - \mu_{x,U}\mu_{y,U}}\left(\frac{\partial^2 w_U}{\partial x^2} + \mu_{y,U}\frac{\partial^2 w_U}{\partial y^2}\right)\left\{\begin{array}{c}-k_{r,\ell e,U}\\+k_{r,te,U}\end{array}\right\}\frac{\partial w_U}{\partial x} = 0 \qquad \text{at} \qquad x = \left\{\begin{array}{c}0\\a\end{array}\right\} \tag{4b}$$

$$\left\{\begin{array}{c}-k_{d,\ell e,U}\\+k_{d,te,U}\end{array}\right\}(w_U - w_L)\left\{\begin{array}{c}+k_{t,\ell e,U}\\-k_{t,te,L}\end{array}\right\}\frac{\partial^2 w_U}{\partial y^2} - \left[\left(2D_{xy,U} + \frac{\mu_{y,U}D_{x,U}}{1 - \mu_{x,U}\mu_{y,U}}\right)\frac{\partial^3 w_U}{\partial x\,\partial y^2}\right.$$

$$\left. + \frac{D_{x,U}}{1 - \mu_{x,U}\mu_{y,U}}\frac{\partial^3 w_U}{\partial x^3} + N_{x,U}\frac{\partial w_U}{\partial x}\right] = 0 \qquad \text{at} \qquad x = \left\{\begin{array}{c}0\\a\end{array}\right\} \tag{4c}$$

7

Lower plate

Replace subscript U by L in equations (4a) and (4b); equation (4c) becomes

$$
\begin{Bmatrix} -k_{d,\ell e,L} \\ +k_{d,te,L} \end{Bmatrix} w_L \begin{Bmatrix} -k_{d,\ell e,U} \\ +k_{d,te,U} \end{Bmatrix} (w_L - w_U) \begin{Bmatrix} +k_{t,\ell e,L} \\ -k_{t,te,L} \end{Bmatrix} \frac{\partial^2 w_L}{\partial y^2} - \left[\left(2D_{xy,L} + \frac{\mu_{y,L} D_{x,L}}{1 - \mu_{x,L}\mu_{y,L}} \right) \frac{\partial^3 w_L}{\partial x \, \partial y^2} \right.
$$

$$
\left. + \frac{D_{x,L}}{1 - \mu_{x,L}\mu_{y,L}} \frac{\partial^3 w_L}{\partial x^3} + N_{x,L} \frac{\partial w_L}{\partial x} \right] = 0 \qquad \text{at} \qquad x = \begin{Bmatrix} 0 \\ a \end{Bmatrix} \tag{4d}
$$

The frequency-independent, linear, hysteretic formulation of structural damping used in reference 6 is employed in the present analysis by modifying all the terms in equations (1), (2), and (4) containing plate bending stiffnesses or spring stiffnesses by an appropriate $(1 + ig)$ factor for simple harmonic motion. This procedure is equivalent to assuming orthotropic structural damping properties as well as orthotropic stiffness properties for both plates and permits arbitrary levels of structural damping to be considered for each of the leading- and trailing-edge support springs as well as for the elastic coupling medium.

Solution

With introduction of the generalized aerodynamic loading terms from equation (3) and of structural damping and with division by the appropriate $D_x / (1 - \mu_x \mu_y)$ term for the upper and lower plates, equations (1) and (2) become

Upper plate

$$
G_{x,U} \frac{\partial^4 w_U}{\partial x^4} + 2 \left(G_{xy,U} \frac{D_{xy,U}}{D_{1,U}} + G_{x,U}\mu_{y,U} \right) \frac{\partial^4 w_U}{\partial x^2 \, \partial y^2} + G_{y,U} \frac{D_{2,U}}{D_{1,U}} \frac{\partial^4 w_U}{\partial y^4} + \frac{N_{x,U}}{D_{1,U}} \frac{\partial^2 w_U}{\partial x^2}
$$

$$
+ \frac{N_{y,U}}{D_{1,U}} \frac{\partial^2 w_U}{\partial y^2} + \frac{\gamma_U}{D_{1,U}} \frac{\partial^2 w_U}{\partial t^2} + \frac{K}{D_{1,U}} \left(w_U - w_L \right) + \frac{\rho c}{D_{1,U}} \frac{\partial w_U}{\partial t} + \frac{2q}{\beta D_{1,U}} \frac{\partial w_U}{\partial x} = 0 \tag{5}
$$

Lower plate

$$G_{x,L} \frac{\partial^4 w_L}{\partial x^4} + 2\left(G_{xy,L} \frac{D_{xy,L}}{D_{1,L}} + G_{x,L}\mu_{y,L}\right) \frac{\partial^4 w_L}{\partial x^2 \partial y^2} + G_{y,L} \frac{D_{2,L}}{D_{1,L}} \frac{\partial^4 w_L}{\partial y^4} + \frac{N_{x,L}}{D_{1,L}} \frac{\partial^2 w_L}{\partial x^2}$$

$$+ \frac{N_{y,L}}{D_{1,L}} \frac{\partial^2 w_L}{\partial y^2} + \frac{\gamma_L}{D_{1,L}} \frac{\partial^2 w_L}{\partial t^2} + \frac{K}{D_{1,L}}\left(w_L - w_U\right) = 0 \tag{6}$$

where the plate stiffness coefficients are defined as

$$D_1 = \frac{D_x}{1 - \mu_x \mu_y} \qquad\qquad D_2 = \frac{D_y}{1 - \mu_x \mu_y} \tag{7}$$

and the damping factors are defined as

$$G_x = 1 + ig_x \qquad G_{xy} = 1 + ig_{xy} \qquad G_y = 1 + ig_y \qquad K = k\left(1 + ig_k\right) \tag{8}$$

Similarly the boundary conditions for the upper plate become

$$w_U(x,y,t) = \frac{\partial^2 w_U(x,y,t)}{\partial y^2} = 0 \qquad \text{at} \qquad y = 0 \text{ and } b \tag{9a}$$

$$G_{x,U}\left(\frac{\partial^2 w_U}{\partial x^2} + \mu_{y,U} \frac{\partial^2 w_U}{\partial y^2}\right) \begin{Bmatrix} -G_{r,\ell e,U} \dfrac{k_{r,\ell e,U}}{D_{1,U}} \\[2mm] +G_{r,te,U} \dfrac{k_{r,te,U}}{D_{1,U}} \end{Bmatrix} \frac{\partial w_U}{\partial x} = 0 \qquad \text{at} \qquad x = \begin{Bmatrix} 0 \\ a \end{Bmatrix} \tag{9b}$$

$$\begin{Bmatrix} -G_{d,\ell e,U} \dfrac{k_{d,\ell e,U}}{D_{1,U}} \\[2mm] +G_{d,te,U} \dfrac{k_{d,te,U}}{D_{1,U}} \end{Bmatrix}\left(w_U - w_L\right) \begin{Bmatrix} +G_{t,\ell e,U} \dfrac{k_{t,\ell e,U}}{D_{1,U}} \\[2mm] -G_{t,te,U} \dfrac{k_{t,te,U}}{D_{1,U}} \end{Bmatrix} \frac{\partial^2 w_U}{\partial y^2} - \left[\left(2G_{xy,U} \frac{D_{xy,U}}{D_{1,U}} + \mu_{y,U}G_{x,U}\right)\right.$$

$$\times \frac{\partial^3 w_U}{\partial x \partial y^2} + G_{x,U} \frac{\partial^3 w_U}{\partial x^3} + \frac{N_{x,U}}{D_{1,U}} \frac{\partial w_U}{\partial x}\Bigg] = 0 \qquad \text{at} \qquad x = \begin{Bmatrix} 0 \\ a \end{Bmatrix} \tag{9c}$$

9

The boundary conditions for the lower plate become

$$w_L(x,y,t) = \frac{\partial^2 w_L(x,y,t)}{\partial y^2} = 0 \quad \text{at} \quad y = 0 \text{ and } b \tag{10a}$$

$$G_{x,L}\left(\frac{\partial^2 w_L}{\partial x^2} + \mu_{y,L}\frac{\partial^2 w_L}{\partial y^2}\right)\left\{\begin{array}{c}-G_{r,le,L}\dfrac{k_{r,le,L}}{D_{1,L}}\\[2mm]+G_{r,te,L}\dfrac{k_{r,te,L}}{D_{1,L}}\end{array}\right\}\frac{\partial w_L}{\partial x} = 0 \quad \text{at} \quad x = \left\{\begin{array}{c}0\\a\end{array}\right\} \tag{10b}$$

$$\left\{\begin{array}{c}-G_{d,le,L}\dfrac{k_{d,le,L}}{D_{1,L}}\\[2mm]+G_{d,te,L}\dfrac{k_{d,te,L}}{D_{1,L}}\end{array}\right\}w_L\left\{\begin{array}{c}-G_{d,le,U}\dfrac{k_{d,le,U}}{D_{1,L}}\\[2mm]+G_{d,te,U}\dfrac{k_{d,te,U}}{D_{1,L}}\end{array}\right\}\left(w_L - w_U\right)\left\{\begin{array}{c}+G_{t,le,L}\dfrac{k_{t,le,L}}{D_{1,L}}\\[2mm]-G_{t,te,L}\dfrac{k_{t,te,L}}{D_{1,L}}\end{array}\right\}\frac{\partial^2 w_L}{\partial y^2}$$

$$-\left[\left(2G_{xy,L}\frac{D_{xy,L}}{D_{1,L}} + \mu_{y,L}G_{x,L}\right)\frac{\partial^3 w_L}{\partial x\, \partial y^2} + G_{x,L}\frac{\partial^3 w_L}{\partial x^3} + \frac{N_{x,L}}{D_{1,L}}\frac{\partial w_L}{\partial x}\right] = 0 \quad \text{at} \quad x = \left\{\begin{array}{c}0\\a\end{array}\right\} \tag{10c}$$

where the complex spring coefficients are defined as

$$\left.\begin{array}{ll}G_{d,le} = 1 + ig_{d,le} & \qquad G_{d,te} = 1 + ig_{d,te}\\[3mm]G_{t,le} = 1 + ig_{t,le} & \qquad G_{t,te} = 1 + ig_{t,te}\\[3mm]G_{r,le} = 1 + ig_{r,le} & \qquad G_{r,te} = 1 + ig_{r,te}\end{array}\right\} \tag{11}$$

For exponentially varying motion of the two plates the assumption of simply supported side edges admits the following lateral deflection w for the two plates as a solution to equations (5) and (6):

$$\left.\begin{array}{l}w_U = X_U \sin\dfrac{\pi y}{b}\, e^{\zeta t}\\[4mm]w_L = X_L \sin\dfrac{\pi y}{b}\, e^{\zeta t}\end{array}\right\} \tag{12}$$

10

where X is the deflection shape in the x-direction and ζ is of the form

$$\zeta = \phi + i\omega \tag{13}$$

Reference 8 has shown that for simple supports along the lateral edges there is no stiffness coupling between cross-stream modes. Use of two-dimensional aerodynamic theory precludes any aerodynamic coupling of orthogonal cross-stream modes; thus, modes with a single half-wave in the cross-stream direction have the lowest natural frequencies and are used to determine the dynamic stability criterion (lowest value of λ for which $\phi > 0$) for the coupled-plate system under consideration.

Substitution of the expressions in equation (12) for w_U and w_L into equations (5) and (6) results in the following two coupled fourth-order ordinary differential equations in X_U and X_L:

$$G_{x,U}X_U^{(4)} + \overline{A}_U X_U'' + \lambda X_U' + \overline{B}_U X_U - \pi^4 S_U X_L = 0 \tag{14}$$

$$G_{x,L}X_L^{(4)} + \overline{A}_L X_L'' + \overline{B}_L X_L - \pi^4 S_L X_U = 0 \tag{15}$$

where the primes denote derivatives with respect to x/a and where

$$\overline{A}_U = \left(\frac{\pi a}{b}\right)^2 \left[R_{x,U} - 2\left(G_{xy,U}\frac{D_{xy,U}}{D_{1,U}} + G_{x,U}\mu_{y,U}\right)\right] \tag{16}$$

$$\left.\begin{aligned}
\overline{B}_U &= \left(\frac{\pi a}{b}\right)^4\left(\frac{\zeta^2}{\omega_{r,U}^2} - R_{y,U} + G_{y,U}\frac{D_{2,U}}{D_{1,U}} + \frac{g_a\zeta}{\omega_{r,U}}\right) + \pi^4 S_U \\[2em]
\overline{B}_L &= \left(\frac{\pi a}{b}\right)^4\left(\frac{\zeta^2}{\omega_{r,L}^2} - R_{y,L} + G_{y,L}\frac{D_{2,L}}{D_{1,L}}\right) + \pi^4 S_L
\end{aligned}\right\} \tag{17}$$

$$\left.\begin{aligned}
S_U &= \frac{Ka^4}{\pi^4 D_{1,U}} & R_{x,U} &= \frac{N_{x,U}b^2}{\pi^2 D_{1,U}} & g_a &= \frac{\rho c}{\gamma_U \omega_{r,U}} \\[1em]
\omega_{r,U}^2 &= \frac{\pi^4 D_{1,U}}{\gamma_U b^4} & R_{y,U} &= \frac{N_{y,U}b^2}{\pi^2 D_{1,U}} & \lambda &= \frac{2qa^3}{\beta D_{1,U}}
\end{aligned}\right\} \tag{18}$$

11

Similar expressions for $\overline{A}_L$, S_L, $\omega^2_{r,L}$, $R_{x,L}$, and $R_{y,L}$ are obtained by replacing subscript U with L in equations (16) and (18).

Equations (14) and (15) may be solved simultaneously for X_U and X_L or combined to yield a single eighth-order ordinary differential equation in X_L as follows. From equation (15),

$$X_U = \frac{1}{\pi^4 S_L}\left(G_{x,L}X_L^{(4)} + \overline{A}_L X_L'' + \overline{B}_L X_L\right) \tag{19}$$

Substitution of the expression in equation (19) for X_U into equation (14) yields the following eighth-order linear homogenous ordinary differential equation in X_L:

$$G_{x,U}G_{x,L}X_L^{(8)} + \left(G_{x,U}\overline{A}_L + G_{x,L}\overline{A}_U\right)X_L^{(6)} + \lambda G_{x,L}X_L^{(5)} + \left(G_{x,U}\overline{B}_L + \overline{A}_U\overline{A}_L + G_{x,L}\overline{B}_U\right)X_L^{(4)}$$

$$+ \lambda\overline{A}_L X_L''' + \left(\overline{A}_U\overline{B}_L + \overline{A}_L\overline{B}_U\right)X_L'' + \lambda\overline{B}_L X_L' + \left(\overline{B}_U\overline{B}_L - \pi^8 S_U S_L\right)X_L = 0 \tag{20}$$

A closed-form solution to equation (20) with constant coefficients may be written

$$X_L = A_1 e^{P_1 x/a} + A_2 e^{P_2 x/a} + \ldots + A_8 e^{P_8 x/a} \tag{21}$$

where the P_i satisfy the characteristic equation

$$G_{x,U}G_{x,L}P_i^8 + \left(G_{x,U}\overline{A}_L + G_{x,L}\overline{A}_U\right)P_i^6 + \lambda G_{x,L}P_i^5 + \left(G_{x,U}\overline{B}_L + \overline{A}_U\overline{A}_L + G_{x,L}\overline{B}_U\right)P_i^4$$

$$+ \lambda\overline{A}_L P_i^3 + \left(\overline{A}_U\overline{B}_L + \overline{B}_U\overline{A}_L\right)P_i^2 + \lambda\overline{B}_L P_i + \left(\overline{B}_U\overline{B}_L - \pi^8 S_U S_L\right) = 0 \tag{22}$$

The boundary conditions for both plates can be written in terms of the P_i and A_i by using equations (12) and (21) along with equations (9) and (10). When written in matrix form the boundary conditions become

$$[\Omega]\{A_i\} = 0 \tag{23}$$

Detailed expressions for the elements of the boundary condition matrix $[\Omega]$ and their derivation are given in the appendix.

12

The flutter behavior of the coupled two-plate system with either aerodynamic or structural damping present is governed by the variation of the complex frequency $\zeta = \phi + i\omega$ as a function of the aerodynamic load λ. Flutter of the system occurs when ϕ becomes positive and, hence, the lowest λ condition when $\phi = 0$ is taken to be the critical condition. This condition corresponds to sustained simple harmonic motion and represents incipient flutter for the system.

Flutter solutions for the coupled two-plate system are obtained as follows. The physical characteristics of the system are specified except for the aerodynamic load λ and the complex frequency ζ. An initial aerodynamic load λ is assumed and then incremented, and values of ζ are determined for each value of λ by an iteration scheme. The iteration on ζ is continued until a set of roots to equation (22) is obtained which satisfies the boundary conditions. Since, in general, the A_i in equations (21) and (23) are not zero, the boundary conditions are satisfied when the determinant of the boundary condition matrix is zero. This process is continued until a value of λ is reached which causes the real part of ζ to be positive by a small value and equation (12) implies that the amplitude of vibration for the system increases without limit. When both aerodynamic and structural damping in the system are zero the real part of ζ (ϕ) is zero for all values of λ below some critical value. When this critical value is reached, two natural frequencies of the system coalesce into complex conjugates, so that positive values of the real part of ζ (ϕ) occur and equation (12) again implies motion with growing amplitude, that is, flutter.

To obtain flutter boundaries for the coupled two-plate system a computer algorithm was written to obtain values of ζ as a function of λ. The algorithm is written in FORTRAN IV for the CDC 6000 series computers at the Langley Research Center and makes use of library subroutines to numerically extract the roots of the eighth-order complex polynomial (eq. (22)) and to evaluate the determinant of the complex boundary condition matrix. In the algorithm, values of ζ which satisfy equation (23) are determined for given values of λ by using a Newton-Raphson iteration scheme wherein a new value of ζ is determined from the current value by the following expression:

$$\zeta_{i+1} = \zeta_i - \frac{\left|\Omega(\zeta_i)\right| \Delta\zeta}{\left|\Omega(\zeta_i)\right| - \left|\Omega(\zeta_i + \Delta\zeta)\right|}$$

where $\Delta\zeta$ is a small increment in ζ used to numerically calculate the first derivative of the determinant of the boundary condition matrix with respect to ζ.

RESULTS AND DISCUSSION

Because of the large number of variables involved, no attempt was made to conduct extensive parametric studies of the flutter behavior of coupled two-plate systems. However, results are presented to show that when aerodynamic and structural damping effects are ignored and the two plates are identical with respect to geometry, inplane loading, edge conditions, and material properties, flutter boundaries can be obtained in terms of the general parameters $\overline{A}$ and $\overline{B}$ as was done in references 8 and 9 for single plates. Some effects of structural damping on the flutter of coupled identical plates for $a/b = 4$ are also presented. In addition, results from the current analysis are compared with results from the modal solutions of references 1 and 2 to assess the validity of these solutions. Two thermal protection systems proposed for space shuttle which can be modeled as coupled two-plate systems are analyzed to determine their flutter characteristics. For each system the stiffnesses of the upper and lower plates differ by 2 orders of magnitude. The plate with low stiffness is exposed to the flow in one system and in the other the plate with high stiffness is exposed to the flow. A discussion of the relative flutter behavior of the two systems is also presented. Finally, the influence on flutter of single plates of unequal support springs at the leading and trailing plate edges is discussed briefly.

Flutter Boundary for Identical Coupled Plates

When aerodynamic and structural damping are neglected and when the two plates are identical with respect to geometry, inplane loading, and material properties, equations (16) and (17) indicate that the respective $\overline{A}$ and $\overline{B}$ parameters for the two plates are equal. For these conditions it is possible to obtain general flutter boundaries for the coupled system for specific stiffness values of the elastic coupling medium and specified boundary conditions. Such flutter boundaries are then applicable to a wide variety of panel configurations, material properties, and inplane loadings.

Although it is possible to generate solutions for various values of the spring stiffness of the coupling medium and for various boundary conditions, only one such solution with both plates simply supported and a coupling-medium spring parameter of $S_U = S_L = 10$ (representative of a lightly coupled system) was obtained to illustrate the nature of such solutions. Figure 2 shows a comparison of the resulting flutter boundary for a coupled two-plate system with a similar boundary for a single plate. The boundaries are shown in terms of $\lambda^{1/3}$ as a function of $\overline{A}$. The anomalous $\lambda = 0$ flutter points occur whenever $\overline{A}$ has a value that causes the two vibration modes which coalesce flutter to have equal natural frequencies for no airflow. For the coupled-plate system the larger number of $\lambda = 0$ flutter points results from the fact that the coupled system has twice the number of natural vibration frequencies associated with a single plate.

14

Eight natural frequencies of the coupled system are shown in figure 3 in which the frequency parameter $\bar{B}$ is shown as a function of $\bar{A}$. The solid curves correspond to vibration modes of the two plates which are in phase, the dashed curves correspond to vibration modes of the two plates which are 180° out of phase, and m denotes the number of half-waves in the stream direction. Shaded regions between any two curves indicate that those modes contiguous to the shaded regions on the plot coalesce to give the lowest value of λ for flutter. As usual in panel flutter, adjacent odd and even modes coalesce for flutter. However, since the coupled-plate system has both in-phase and out-of-phase vibration modes, many possibilities exist for coalescence of multiple pairs of modes which have nearly the same degree of frequency separation, and it is not obvious which pair will give the lowest flutter value of λ. Comparison of figures 2 and 3 indicates that the $\lambda = 0$ flutter points coincide with crossings of frequencies which coalesce for flutter and that the multiplicity of these points results from the double set of frequencies.

Although variation of the coupling-medium spring parameter S is not expected to change the basic character of the flutter boundary for the two-plate system, such changes will influence the separation of the in-phase and out-of-phase natural frequencies for the system and hence the $\bar{A}$ values at which the $\lambda = 0$ flutter points occur. Reference 6 shows that inclusion of aerodynamic and structural damping in the theory can remove the $\lambda = 0$ flutter points for single plates. Calculations were made to determine whether the same effects hold for a coupled two-plate system. However, since inclusion of damping precludes a flutter solution in terms of the general parameters $\bar{A}$ and $\bar{B}$, it is necessary to pick a specific plate configuration. Thus, an a/b = 4 coupled-plate system is used to illustrate the effects of aerodynamic and structural damping on the flutter of coupled plates. Flutter boundaries for such a system with $S_U = S_L = 10$ are shown in figure 4 in which $\lambda^{1/3}$ is shown as a function of the inplane loading parameter R_x. The dashed boundary is for no damping and the solid boundary is for structural damping coefficients g_x, g_{xy}, and g_y of 0.01 in the plates and aerodynamic damping corresponding to sea level conditions. The aerodynamic damping is based on a 0.051-cm (0.02-in.) thick aluminum plate and sea level air properties and was calculated from the following equation from reference 6:

$$g_a = \frac{1}{\pi^2}\left(\frac{\rho \beta^2}{cM^4}\right)^{1/3}\left(\frac{D_{1,U}}{\gamma_U^{\ 3}}\right)^{1/6}\lambda^{2/3}$$

The damping has a strong smoothing effect on the flutter boundary and completely removes the $\lambda = 0$ flutter points. Although on the basis of these a/b = 4 results, it appears that damping has a large stabilizing effect and removes the $\lambda = 0$ flutter points for both one- and two-plate systems, such is not always the case. For example, reference 10 shows

that structural damping is destabilizing for built-up plates with low a/b ratios (approximately 1). Limited results concerning such behavior are discussed in a subsequent section.

Comparison of Modal and Closed-Form Results

References 1 and 2 present results from two-mode Galerkin solutions for a coupled two-plate system with $a/b = 1$, simple support boundary conditions, and a value of the coupling-medium spring parameter $S_U = S_L = S = 20$. Reference 2 also presents a flutter boundary for $S = 10$. In figure 5(a), results from both analyses are compared with closed-form results from the present analysis. Flutter boundaries for identical plates with identical inplane loading are shown in terms of λ as a function of the inplane loading parameter R_X. These results are for $S = 20$. Closed-form results are shown by the solid curve and modal results are shown by the dashed curve (ref. 1) and by the circular symbols (ref. 2). A closed-form boundary for a single plate is shown for reference. As mentioned in reference 2, for some as yet unexplained reason the two modal solutions from references 1 and 2 do not agree, although both employ the same representation of the mode shapes. The two-mode Galerkin solutions have the correct trends but tend to be unconservative for some values of R_X. Results for $S = 10$ are shown in figure 5(b) and again the two-mode solution has the correct trend, but it shows a tendency toward conservatism in some regions particularly as R_X increases negatively. The results of figure 5 indicate that as S increases from 10 to 20, the first $\lambda = 0$ flutter point shifts to a negative (tensile) value of R_X. As mentioned in reference 2, inclusion of aerodynamic damping will remove the anomalous $\lambda = 0$ flutter point; but as indicated on figure 5(a), the boundary continues to exhibit a large dip in the vicinity of $R_X = -7$. Calculations from the closed-form solution showed the same trends, and when structural damping was included in the calculations, no appreciable effect was found at the $\lambda = 0$ flutter points; however, the structural damping was found to be destabilizing for other values of R_X. As mentioned previously, this destabilizing effect has been noted for single plates in reference 10 and was not pursued further in the current investigation.

Reference 1 also presents results for two geometrically identical plates with only one plate subjected to inplane loading. These results are compared with closed-form results in figure 6. Again $a/b = 1$, $S = 20$, and both plates are simply supported. Figure 6(a) shows flutter boundaries for the upper plate only subjected to inplane loading and figure 6(b) shows similar boundaries for the lower plate subjected to inplane loading. Solid curves denote closed-form results and dashed curves denote two-mode results. In this instance the two-mode solutions are for the most part unconservative and in the region of negative R_X do not exhibit correct trends of the closed-form solution. Examination of figure 7, which shows the natural frequencies of the coupled two-plate system with only one plate subjected to inplane loading, reveals the reason for this behavior.

Shaded regions denote that those modes contiguous to the shaded regions coalesce for flutter. Since the two-mode solution is restricted to the first two modes, it can give reliable results only when these modes coalesce for flutter. Thus, the disparity between the exact and two-mode solutions results from the fact that the boundary for the upper plate subjected to inplane loading (fig. 6(a)), except for $R_X < -19$ and $R_X > 6.5$ (fig. 7), is governed by a coalescence involving the third natural frequency. When the lower plate is subjected to inplane loading (fig. 6(b)), the flutter boundary from $R_X = -13$ to 0 is governed by a coalescence involving modes 1 and 2, and although the two-mode solution is unconservative, the trend is correct. Outside the region $R_X = -13$ to 0, mode 3 is again involved and the disparity between the two-mode and closed-form solutions worsens.

Application to Proposed Thermal Protection Systems

Flexible mat system.- In reference 11 a thermal protection system (TPS) is proposed which consists of a flexible mat fabricated from fibrous ceramic felt layers covered by a dense ceramic coating bonded to a load carrying primary structure. Since no flutter results for this TPS were presented in reference 11, the present study was undertaken. The TPS was modeled as a system of springs connecting the surface covering to the substructure, and calculations were made to determine the flutter characteristics for such TPS. The system, shown in figure 8, is similar to that considered in figure 6(b) with the exception that the plate exposed to the flow has a much lower flexural stiffness than the unexposed plate and the ends of the exposed plate are not necessarily simply supported.

Flutter boundaries which were calculated for this system on the assumption that it behaves as two spring-connected beams are also shown in figure 8. The solid curves represent flutter boundaries for beams of finite stiffness. The upper boundary results from the assumption that the leading and trailing edges of both beams are simply supported. The lower boundary corresponds to the assumption that the leading and trailing edges of the upper beam are supported by deflectional springs with a spring stiffness equal to that of the coupling medium. The two horizontal dashed curves correspond to similar boundary conditions but with the lower beam of infinite bending stiffness.

Figure 9 shows the natural frequencies of the two-beam system as a function of the inplane loading in the lower beam. The solid curves are for simple supports and in-phase motion, the dashed curve is the first out-of-phase mode for simple supports, and the dot-dashed curves are for spring supported edges and in-phase motion. Shaded regions between any two curves indicate that those modes contiguous to the shaded regions coalesce for flutter. Again the difference in the two flutter boundaries is related to the modes which coalesce for flutter. Along the boundary for simple supports, in-phase modes 1 and 2 coalesce for flutter up to $R_X/R_{X,cr} = 0.5$; between $R_X/R_{X,cr} = 0.5$ and approximately 0.67, in-phase modes 2 and 3 coalesce; and beyond $R_X/R_{X,cr} = 0.67$, in-phase mode 2 and out-of-phase mode 1 coalesce for flutter. For the boundary corre-

sponding to spring supports, in-phase modes 2 and 3 coalesce along the entire boundary to give the flutter condition. For this structure the upper beam has low flexural stiffness and the lower beam has high flexural stiffness (2 orders of magnitude greater than the upper). For both sets of boundary conditions it is interesting to note that if the stiffness of the lower beam is considered to be infinite, conservative predictions of λ result which are in good agreement with the corresponding minimum values of λ obtained for a lower beam of finite stiffness. This suggests that for configurations in which the lower beam carries the inplane loading and is very stiff in relation to the upper beam, use of the simpler solution may be acceptable.

Reusable surface insulation.- Reference 3 presents a modal solution for the flutter behavior of a proposed space shuttle TPS consisting of relatively thick ceramic tiles mounted on a soft viscoelastic foundation which is bonded to a primary load carrying metallic structure. The concept is usually referred to as a reusable surface insulation (RSI) TPS. A Rayleigh-Ritz flutter solution employing 4 free-free beam streamwise modes and 1 free-free beam cross-stream mode per tile, and 12 simply supported plate streamwise modes and up to 3 simply supported plate cross-stream modes for the metallic primary structure was obtained.

The structural model in reference 3 for the viscoelastic foundation neglects viscous effects of the foundation material but is classified as a shear model (in contrast to the Winkler model) in that a point load gives rise not only to a deflection at that point but to surrounding points as well with an exponential decay of deflection away from the point of application of the force. In reference 3, the Winkler model and shear model were found to give essentially the same results for a single tile and for streamwise multiple tile arrays when the viscoelastic foundation was assumed to be cut between tiles. The cut in the foundation is a part of the space shuttle design; hence, the difference in foundation models does not preclude valid comparisons of results from the present analysis with results from reference 3. Other differences also exist between the two analyses. For instance, the analysis of reference 3 is applicable to multitile arrays and assumes the tiles to be free on all edges. The current analysis, however, is restricted to a single two-plate combination which is simply supported along the side edges. Thus, the two analyses can be compared only on a limited basis. One valid comparison is for $a/b = 0$. Reference 3 gives a flutter value for λ of 65 for a two-plate system where the RSI tile has a flexural stiffness of 52 N-m (458 lb-in.), the foundation has coupling-medium spring parameters of $S_U = 32$ and $S_L = 1971$, the lower plate has a flexural stiffness of 0.75 N-m (6.67 lb-in.), the plates are 51 cm (20 in.) long, and sea level aerodynamic damping is included. The present analysis gives a value of λ of 56 for similar conditions.

An additional comparison with results from reference 3 is shown in figure 10 in which flutter boundaries are given for an $a/b = 4$ coupled-plate system. Since refer-

ence 3 assumes the tile to be free on all edges, the upper plate was modeled for the current analysis as having stiffness in the streamwise direction only and hence is a beam-type representation of the actual tile. The flutter boundaries shown in figure 10 are presented in terms of λ as a function of $R_x/R_{x,cr}$ where $R_{x,cr}$ is the value of the inplane loading parameter required to buckle the lower plate alone. Structural details of the coupled system are shown in the inset in figure 10. Two boundaries from reference 3 are shown; the boundary labeled $n = 1$ is for a single tile, and the curve labeled $n = 4$ is for a streamwise array of four tiles. The boundary labeled closed-form solution is from the present analysis and agrees best with the $n = 4$ boundary from reference 3. The apparent lack of agreement between the closed-form and modal results for $n = 1$ may be due to the relatively small number of modes used to describe the motion of the tile. Two rigid-body and two bending modes may not be sufficient to adequately describe the motion of the tiles for $n = 1$.

Results from the closed-form solution indicate that, although the mass of the upper plate is approximately twice that of the lower plate and the stiffness of the upper plate is two orders of magnitude greater than that of the lower plate, the coupling between the two plates is sufficient to cause the upper plate to respond predominately in bending rather than as a rigid body. The better agreement between the closed-form $n = 1$ and modal $n = 4$ flutter boundaries can be attributed to the closeness of the mode shapes for the respective solutions. Figure 11 shows mode shapes for the first two modes of the coupled system. Since those are the modes which coalesce for flutter, it can be expected that the two solutions might give similar flutter results. Reference 3 points out that the salient feature of this coupled system is that although the upper plate has a greater mass and a much higher stiffness than the lower plate, it is the flexibility of the lower plate which governs the response of the system. In fact, the addition of the upper plate and elastic coupling medium actually results in an increase in the dynamic pressure required to flutter the coupled system over that required to flutter the lower plate alone $\left(q/\beta_{coupled} = 172 \text{ kPa (25 psi)} \quad \text{and} \quad q/\beta_{single} = 26 \text{ kPa (4 psi)} \right)$. The opposite behavior occurs for the situation shown in figure 8 in which the upper plate has a much lower flexural stiffness (two orders of magnitude) than the lower plate $\left(q/\beta_{coupled} = 834 \text{ kPa} \right.$ (121 psi) and $q/\beta_{single} = 105 \text{ MPa } (15\ 290 \text{ psi}) \Big)$. In addition, the presence of the RSI tiles and viscoelastic foundation increases the buckling load for the coupled system over that for the lower plate alone.

Single plates with unequal supports.- As mentioned in reference 4, metallic thermal protection systems have been proposed which can have rows of continuous supports with widely varying flexibilities normal to the plane of the panel. To illustrate the effects on flutter of such unequal deflectional supports, calculations were made using the present analysis for single plates with large streamwise bending stiffness and essentially zero

cross-stream bending and twisting stiffnesses. Figure 12 shows stability boundaries in terms of λ as a function of spring stiffness ratios $k_{d,te}/k_{d,\ell e}$ from 0 to 1.0 and $k_{d,te}/k_{d,\ell e}$ from 1.0 to 0. The stability boundaries are for constant values of the spring stiffness parameter $K_{d,\ell e}$ of 100, 10, and 1. The dashed curve, shown for comparison, is the value of λ for infinite spring stiffness or simple supports.

The curves show large reductions in λ from the value associated with simple supports as the edge spring stiffness is decreased. The effect of unequal supports appears to be a function of $K_{d,\ell e}$. For example, when $K_{d,\ell e}$ is large (e.g., 100), the effect of reducing the trailing-edge spring stiffness is small as shown for $k_{d,te}/k_{d,\ell e} < 1$. However, when $K_{d,\ell e}$ is small (e.g., 1), a large reduction in the flutter λ occurs as the trailing-edge spring stiffness decreases. Additionally, when $K_{d,\ell e}$ is small, large values of the trailing-edge spring stiffness $\left(k_{d,\ell e}/k_{d,te} < 1\right)$ may introduce divergence (loss of static stability) which also results in large reductions in λ.

On the basis of the results presented in figure 12, it appears that in the design of a TPS which employs flexible edge supports to alleviate thermal stresses, adequate attention must be given to the design of the supports to preclude the drastic reductions of aeroelastic stability margins associated with unequal supports.

CONCLUDING REMARKS

Flutter of two parallel elastically coupled plates was investigated analytically. A closed-form solution including both aerodynamic and hysteretic structural damping was presented for supersonic flutter of flat orthotropic plates coupled by an elastic medium. Both plates were simply supported along the side edges but were supported by deflectional, rotational, and torsional springs of arbitrary stiffness at the leading and trailing edges. Two-dimensional quasi-steady aerodynamics was used in the analysis.

Because of the large number of variables involved, no attempt was made to conduct extensive parametric studies of the flutter behavior for coupled two-plate systems. However, selected results were presented to illustrate the general flutter nature of such systems. Similar to results for single plates, anomalous zero-dynamic-pressure flutter points were predicted for the two-plate system whenever the frequencies which coalesce for flutter were equal for no airflow. Inclusion of aerodynamic and structural damping in the calculation removed the computed anomalous zero-dynamic-pressure flutter points for the two-plate system for high length-width ratios (approximately 4) but had little effect for low length-width ratios (approximately 1).

A comparison of flutter results was made for two thermal protection systems proposed for space shuttle. The two systems were similar in that for each the coupled plates

differed in flexural stiffness by two orders of magnitude. The two systems differed in that for one the plate of higher flexural stiffness was exposed to the airflow and in the other the plate of lower flexural stiffness was exposed to the airflow. The comparison of flutter results revealed that for coupled two-plate systems with different flexural stiffnesses in the two plates, maximum flutter margins occur when the plate with the higher flexural stiffness is exposed to the flow.

Finally, on the basis of flutter results presented for a single plate with unequal deflectional supports, it appears that for thermal protection systems which employ flexible edge supports to alleviate thermal stresses, adequate attention must be given to the design of the supports to preclude the drastic reductions in aeroelastic stability margins associated with unequal supports.

Langley Research Center
National Aeronautics and Space Administration
Hampton, Va. 23665
November 4, 1975

APPENDIX

BOUNDARY CONDITION MATRIX

The boundary conditions are given by equations (9) and (10) in the main text. Equation (12), which is assumed to satisfy equations (5) and (6), satisfies exactly boundary conditions (9a) and (10a) and is repeated for convenience; that is,

$$w_U = X_U \sin \frac{\pi y}{b} e^{\zeta t}$$

$$w_L = X_L \sin \frac{\pi y}{b} e^{\zeta t}$$

These expressions modify the remaining boundary conditions (eqs. (9b), (9c), (10b), and (10c)) as follows:

Upper plate

$$G_{x,U}\left(X_U'' - \mu_{y,U}\frac{\pi^2 a^2}{b^2}X_U\right)\begin{Bmatrix} -G_{r,\ell e,U}K_{r,\ell e,U} \\ +G_{r,te,U}K_{r,\ell e,U} \end{Bmatrix}X_U' = 0 \quad \text{at} \quad x = \begin{Bmatrix} 0 \\ a \end{Bmatrix}$$

$$\begin{Bmatrix} -G_{d,\ell e,U}K_{d,\ell e,U} \\ +G_{d,te,U}K_{d,te,U} \end{Bmatrix}(X_U - X_L)\begin{Bmatrix} -G_{t,\ell e,U}K_{t,\ell e,U} \\ +G_{t,te,U}K_{t,te,U} \end{Bmatrix}\frac{\pi^2 a^2}{b^2}X_U - \left[G_{x,U}X_U''' \right.$$

$$\left. -\left(\frac{\pi a}{b}\right)^2\left(2G_{xy,U}\frac{D_{xy,U}}{D_{1,U}} + G_{x,U}\mu_{y,U} - R_{x,U}\right)X_U'\right] = 0 \quad \text{at} \quad x = \begin{Bmatrix} 0 \\ a \end{Bmatrix} \tag{A1}$$

Lower plate

$$G_{x,L}\left(X_L'' - \mu_{y,L}\frac{\pi^2 a^2}{b^2}X_L\right)\begin{Bmatrix} -G_{r,\ell e,L}K_{r,\ell e,L} \\ +G_{r,te,L}K_{r,te,L} \end{Bmatrix}X_L' = 0 \quad \text{at} \quad x = \begin{Bmatrix} 0 \\ a \end{Bmatrix}$$

$$\begin{Bmatrix} -G_{d,\ell e,L}K_{d,\ell e,L} \\ +G_{d,te,L}K_{d,te,L} \end{Bmatrix}X_L\begin{Bmatrix} -G_{d,\ell e,U}\overline{K}_{d,\ell e,U} \\ +G_{d,te,U}\overline{K}_{d,te,U} \end{Bmatrix}(X_L - X_U)\begin{Bmatrix} -G_{t,\ell e,L}K_{t,\ell e,L} \\ +G_{t,te,L}K_{t,te,L} \end{Bmatrix}\frac{\pi^2 a^2}{b^2}X_L$$

$$-\left[G_{x,L}X_L''' - \left(\frac{\pi a}{b}\right)^2\left(2G_{xy,L}\frac{D_{xy,L}}{D_{1,L}} + G_{x,L}\mu_{y,L} - R_{x,L}\right)X_L'\right] = 0 \quad \text{at} \quad x = \begin{Bmatrix} 0 \\ a \end{Bmatrix} \tag{A2}$$

22

APPENDIX

where

$$K_{d,le,U} = \frac{k_{d,le,U}a^3}{D_{1,U}} \qquad\qquad K_{d,te,U} = \frac{k_{d,te,U}a^3}{D_{1,U}}$$

$$K_{r,le,U} = \frac{k_{r,le,U}a}{D_{1,U}} \qquad\qquad K_{r,te,U} = \frac{k_{r,te,U}a}{D_{1,U}}$$

$$K_{t,le,U} = \frac{k_{t,le,U}a}{D_{1,U}} \qquad\qquad K_{t,te,U} = \frac{k_{t,te,U}a}{D_{1,U}}$$

These expressions for the lower plate may be obtained by replacing subscript U with L. Finally,

$$\overline{K}_{d,le,U} = \frac{k_{d,te,U}a^3}{D_{1,L}} \qquad\qquad \overline{K}_{d,te,U} = \frac{k_{d,te,U}a^3}{D_{1,L}}$$

Equations (19) and (21) from the main text (repeated here for convenience) are

$$X_U = \frac{1}{\pi^4 S_L}\left(G_{x,L}X_L^{(4)} + \overline{A}_L X_L'' + \overline{B}_L X_L\right)$$

$$X_L = A_1 e^{P_1\, x/a} + A_2 e^{P_2\, x/a} + \ldots + A_8 e^{P_8\, x/a}$$

With these equations the boundary conditions given by equations (A1) and (A2) may be written as follows:

Upper plate

$$\sum_{j=1}^{8}\left(G_{x,U}\left[P_j^2 - \mu_{y,U}\left(\frac{\pi a}{b}\right)^2\right]\begin{Bmatrix}-G_{r,le,U}K_{r,le,U}\\ +G_{r,te,U}K_{r,te,U}\end{Bmatrix}P_j\right)\alpha_j A_j e^{P_j\, x/a} = 0 \quad \text{at} \quad x = \begin{Bmatrix}0\\ a\end{Bmatrix} \qquad (A3a)$$

23

$$\sum_{j=1}^{8} \left[\left\{ \begin{matrix} -G_{d,\ell e,U}K_{d,\ell e,U} \\ +G_{d,te,U}K_{d,te,U} \end{matrix} \right\} (\alpha_j - 1) \left\{ \begin{matrix} -G_{t,\ell e,U}K_{t,\ell e,U} \\ +G_{t,te,U}K_{t,te,U} \end{matrix} \right\} \left(\frac{\pi a}{b}\right)^2 \alpha_j - \left(G_{x,U}P_j^3 + \left(\frac{\pi a}{b}\right)^2 \left[R_{x,U} \right. \right. \right.$$

$$\left. \left. \left. - \left(2G_{xy,U} \frac{D_{xy,U}}{D_{1,U}} + G_{x,U}\mu_{y,U} \right) \right] P_j \right) \alpha_j \right] A_j e^{P_j \, x/a} = 0 \quad \text{at} \quad x = \left\{ \begin{matrix} 0 \\ a \end{matrix} \right\} \qquad \text{(A3b)}$$

Lower plate

$$\sum_{j=1}^{8} \left(G_{x,L}\left[P_j^2 - \mu_{y,L}\left(\frac{\pi a}{b}\right)^2 \right] \left\{ \begin{matrix} -G_{r,\ell e,L}K_{r,\ell e,L} \\ +G_{r,te,L}K_{r,te,L} \end{matrix} \right\} P_j \right) A_j e^{P_j \, x/a} = 0 \quad \text{at} \quad x = \left\{ \begin{matrix} 0 \\ a \end{matrix} \right\} $$

$$\sum_{j=1}^{8} \left[\left\{ \begin{matrix} -G_{d,\ell e,L}K_{d,\ell e,L} - G_{d,\ell e,U}\overline{K}_{d,\ell e,U} \\ +G_{d,te,L}K_{d,te,L} + G_{d,te,U}\overline{K}_{d,te,U} \end{matrix} \right\} (1 - \alpha_j) \left\{ \begin{matrix} -G_{t,\ell e,L}K_{t,\ell e,L} \\ +G_{t,te,L}K_{t,te,L} \end{matrix} \right\} \left(\frac{\pi a}{b}\right)^2 - \left(G_{x,L}P_j^3 \right. \right. \quad \text{(A4)}$$

$$\left. \left. + \left(\frac{\pi a}{b}\right)^2 \left[R_{x,L} - \left(2G_{xy,L} \frac{D_{xy,L}}{D_{1,L}} + G_{x,L}\mu_{y,L} \right) \right] P_j \right) \right] A_j e^{P_j \, x/a} = 0 \quad \text{at} \quad x = \left\{ \begin{matrix} 0 \\ a \end{matrix} \right\}$$

where

$$\alpha_j = \frac{1}{\pi^4 S_L} \left(G_{x,L}P_j^4 + \overline{A}_L P_j^2 + \overline{B}_L \right) \qquad \text{(A5)}$$

For $j = 1, 2, 3, \ldots, 8$. The eight equations given by equations (A3) and (A4) can be combined and written in matrix form as follows:

$$[\Omega]\left\{A\right\} = 0 \qquad \text{(A6)}$$

where $[\Omega]$ is a 8×8 square matrix and $\{A\}$ is a 8×1 column matrix. The elements of $[\Omega]$ are given by the following expressions:

$$\Omega_{1,j} = \left\{ G_{x,U}\left[P_j^2 - \mu_{y,U}\left(\frac{\pi a}{b}\right)^2\right] - G_{r,\ell e,U}K_{r,\ell e,U}P_j \right\}\alpha_j$$

$$\Omega_{2,j} = \left\{ G_{x,U}\left[P_j^2 - \mu_{y,U}\left(\frac{\pi a}{b}\right)^2\right] + G_{r,te,U}K_{r,te,U}P_j \right\}\alpha_j e^{P_j}$$

$$\Omega_{3,j} = -G_{d,\ell e,U}K_{d;\ell e,U}\left(\alpha_j - 1\right) - G_{t,\ell e,U}K_{t,\ell e,U}\left(\frac{\pi a}{b}\right)^2\alpha_j - \left\{ G_{x,U}P_j^3 + \left(\frac{\pi a}{b}\right)^2\left[R_{x,U}\right.\right.$$
$$\left.\left. - \left(2G_{xy,U}\frac{D_{xy,U}}{D_{1,U}} + G_{x,U}\mu_{y,U}\right)\right]P_j \right\}\alpha_j$$

$$\Omega_{4,j} = \left(G_{d,te,U}K_{d,te,U}\left(\alpha_j - 1\right) + G_{t,te,U}K_{t,te,U}\left(\frac{\pi a}{b}\right)^2\alpha_j - \left\{ G_{x,U}P_j^3 + \left(\frac{\pi a}{b}\right)^2\left[R_{x,U}\right.\right.\right.$$
$$\left.\left.\left. - \left(2G_{xy,U}\frac{D_{xy,U}}{D_{1,U}} + G_{x,U}\mu_{y,U}\right)\right]P_j \right\}\alpha_j \right)e^{P_j}$$

$$\Omega_{5,j} = G_{x,L}\left[P_j^2 - \mu_{y,L}\left(\frac{\pi a}{b}\right)^2\right] - G_{r,\ell e,L}K_{r,\ell e,L}P_j$$

$$\Omega_{6,j} = \left\{ G_{x,L}\left[P_j^2 - \mu_{y,L}\left(\frac{\pi a}{b}\right)^2\right] + G_{r,te,L}K_{r,te,L}P_j \right\}e^{P_j}$$

$$\Omega_{7,j} = -G_{d,\ell e,L}K_{d,\ell e,L} - G_{d,\ell e,U}\overline{K}_{d,\ell e,U}\left(1 - \alpha_j\right) - G_{t,\ell e,L}K_{t,\ell e,L}\left(\frac{\pi a}{b}\right)^2 - \left\{ G_{x,L}P_j^3\right.$$
$$\left. + \left(\frac{\pi a}{b}\right)^2\left[R_{x,L} - \left(2G_{xy,L}\frac{D_{xy,L}}{D_{1,L}} + G_{x,L}\mu_{y,L}\right)\right]P_j \right\}$$

$$\Omega_{8,j} = \left(G_{d,te,L}K_{d,te,L} + G_{d,te,U}\overline{K}_{d,te,U}\left(1 - \alpha_j\right) + G_{t,te,L}K_{t,te,L}\left(\frac{\pi a}{b}\right)^2 - \left\{ G_{x,L}P_j^3\right.\right.$$
$$\left.\left. + \left(\frac{\pi a}{b}\right)^2\left[R_{x,L} - \left(2G_{xy,L}\frac{D_{xy,L}}{D_{1,L}} + G_{x,L}\mu_{y,L}\right)\right]P_j \right\}\right)e^{P_j}$$

$$(A7)$$

for $j = 1, 2, 3, \ldots, 8$.

REFERENCES

1. McElman, John A.: Flutter of Two Parallel Flat Plates Connected by an Elastic Medium. AIAA J., vol. 2, no. 2, Feb. 1964, pp. 377-379.

2. Johns, D. J.; and Taylor P. W.: Vibration and Flutter of Parallel Flat Plates Connected by an Elastic Medium. AIAA/ASME 11th Structures, Structural Dynamics, and Materials Conference, Apr. 1970, pp. 25-35.

3. Dowell, Earl H.: Vibration and Flutter Analysis of Reusable Surface Insulation Panels. J. Spacecraft & Rockets, vol. 12, no. 1, Jan. 1975, pp. 44-50.

4. Bohon, Herman L.; and Shore, Charles P.: Application of Recent Panel Flutter Research to the Space Shuttle. Part II — Influence of Edge Clips and Flow Angularity. NASA Space Shuttle Technology Conference, Volume III — Dynamics and Aeroelasticity, NASA TM X-2274, 1971, pp. 247-264.

5. Dixon, Sidney C.: Comparison of Panel Flutter Results From Approximate Aerodynamic Theory With Results From Exact Inviscid Theory and Experiment. NASA TN D-3649, 1966.

6. Shore, Charles P.: Effects of Structural Damping on Flutter of Stressed Panels. NASA TN D-4990, 1969.

7. Libove, Charles; and Batdorf, S. B.: A General Small-Deflection Theory for Flat Sandwich Plates. NACA Rep. 899, 1948. (Supersedes NACA TN 1526.)

8. Hedgepeth, John M.: Flutter of Rectangular Simply Supported Panels at High Supersonic Speeds. J. Aeronaut. Sci., vol. 24, no. 8, Aug. 1957, pp. 563-573, 586.

9. Erickson, Larry L.: Supersonic Flutter of Flat Rectangular Orthotropic Panels Elastically Restrained Against Edge Rotation. NASA TN D-3500, 1966.

10. Hess, Robert W.: Experimental and Analytical Investigation of the Flutter of Flat Built-Up Panels Under Streamwise Inplane Load. NASA TR R-330, 1970.

11. Alexander, J. G.: A Non Rigid Reusable Surface Insulation Concept for the Space Shuttle Thermal Protection System. Symposium on Reusable Surface Insulation for Space Shuttle, Volume III — Thermal Protection System Design and Optimization, NASA TM X-2721, 1973, pp. 1185-1225.
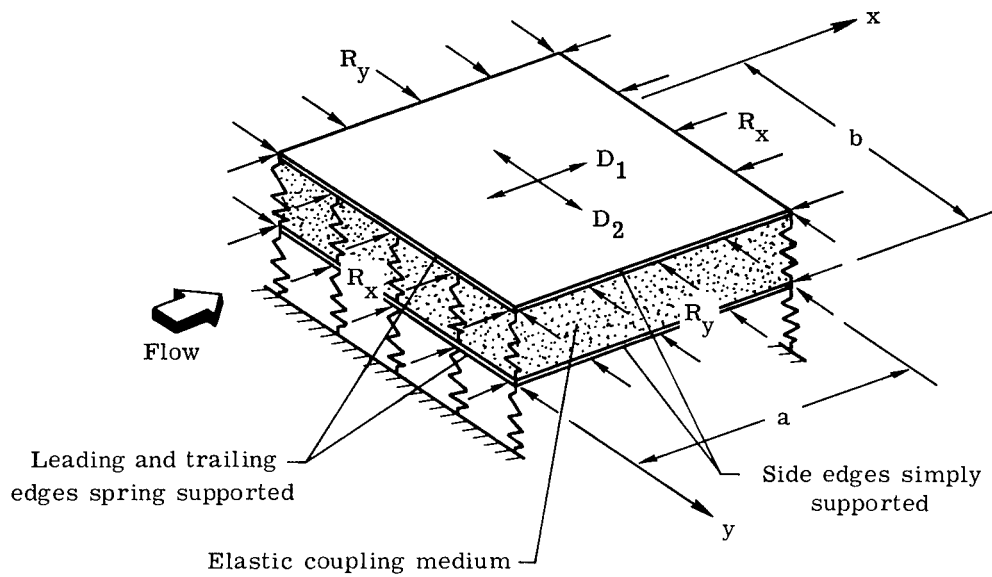
(a) Coupled-plate configuration.

Deflectional and rotational springs

Torsional springs
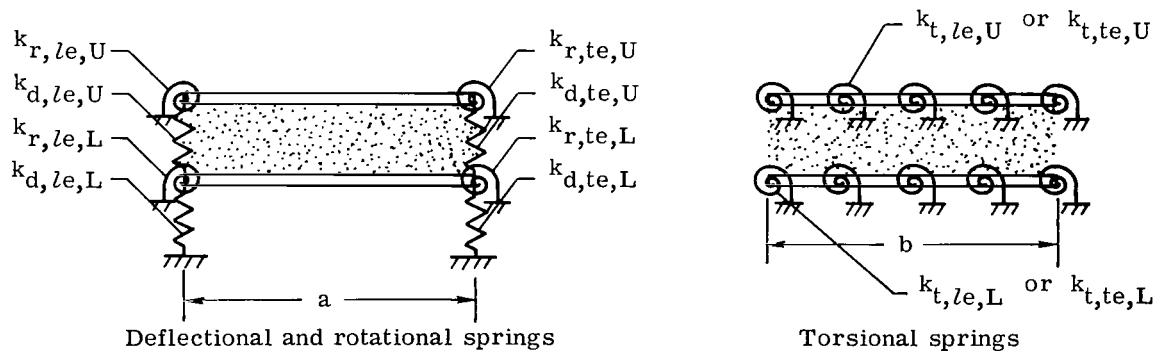
(b) Schematic of spring supports.

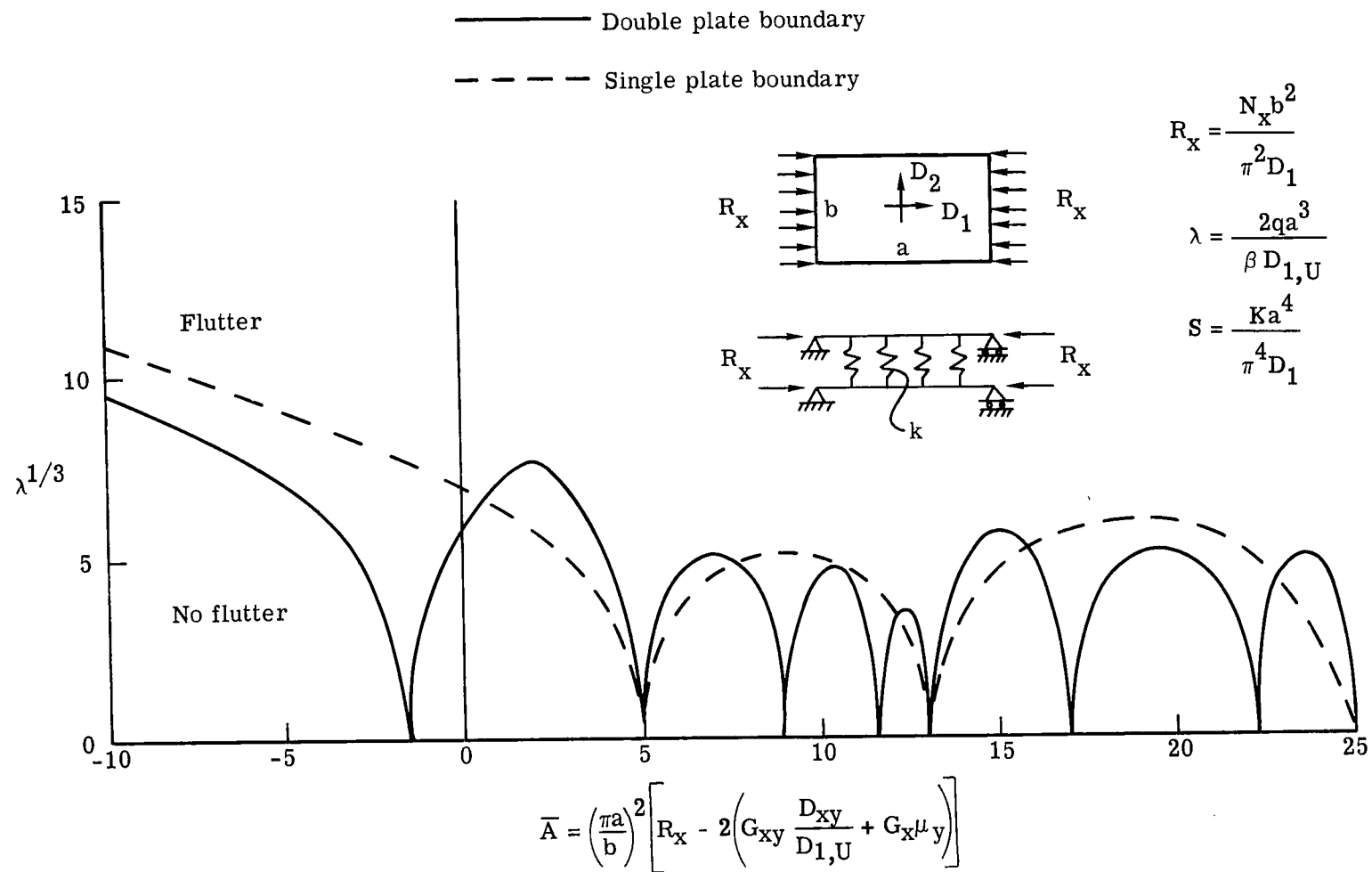Figure 1.- Coupled plates, coordinate system, and spring support system.

Figure 2.- Flutter boundaries for parallel elastically coupled identical plates and for a single plate;   S = 10; no structural and aerodynamic damping.
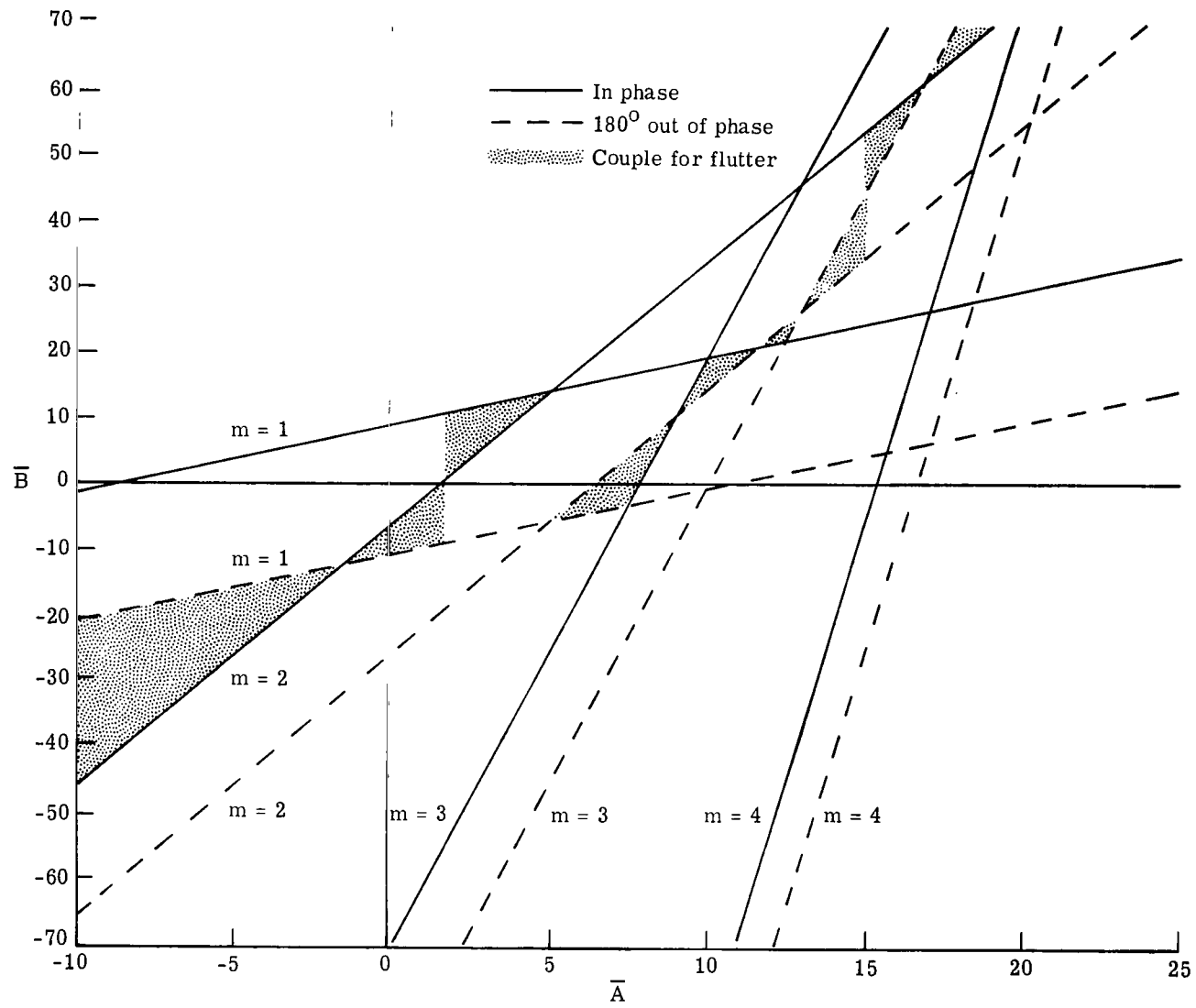
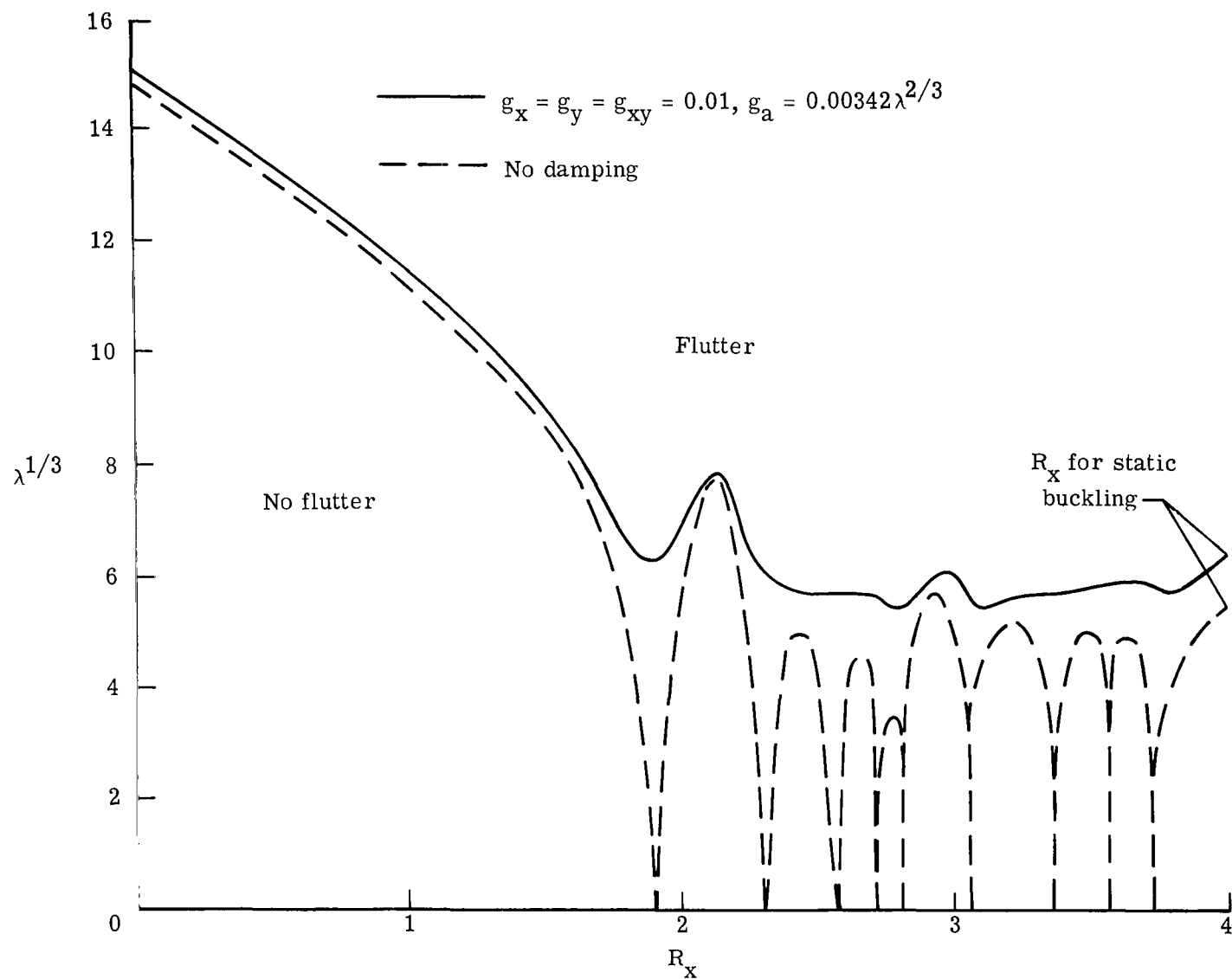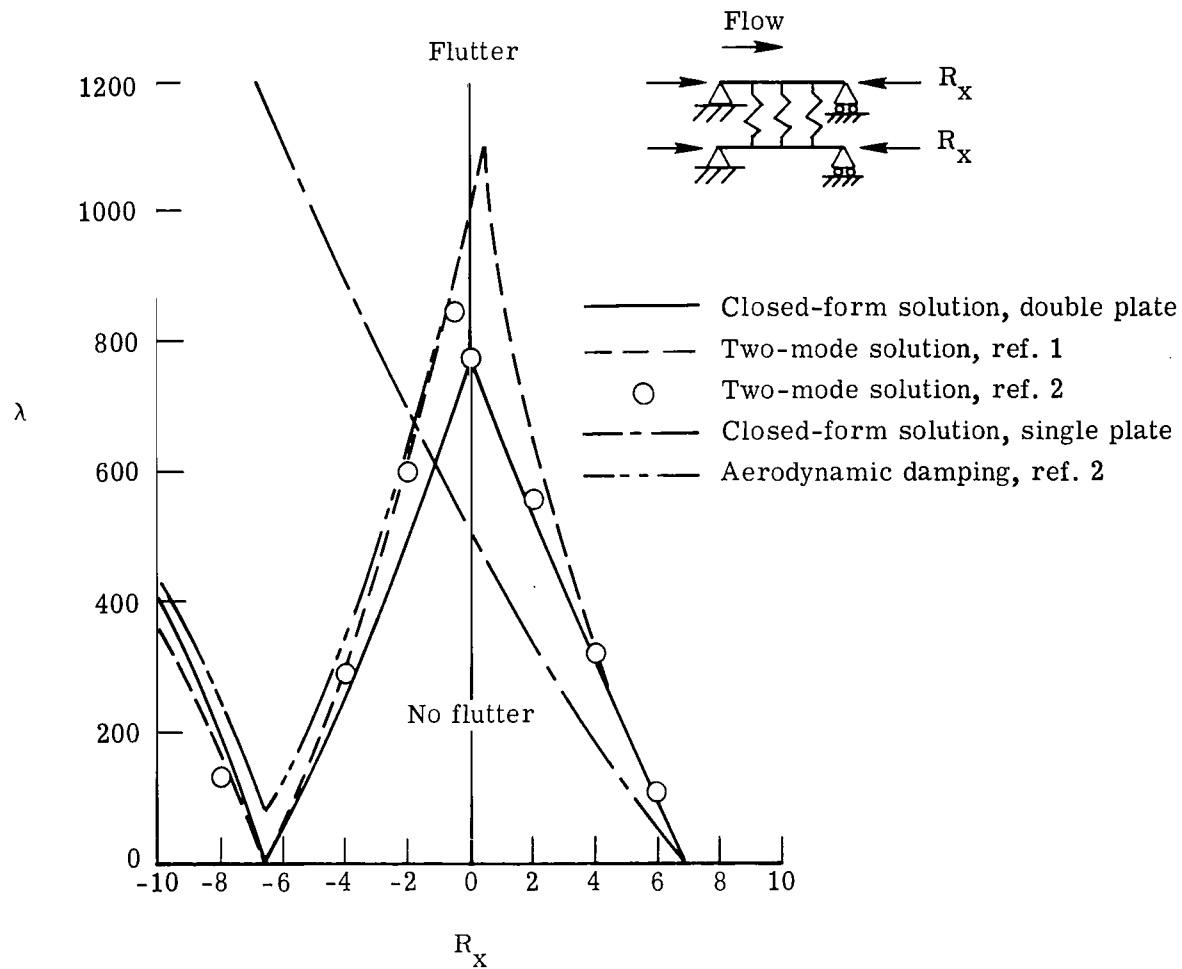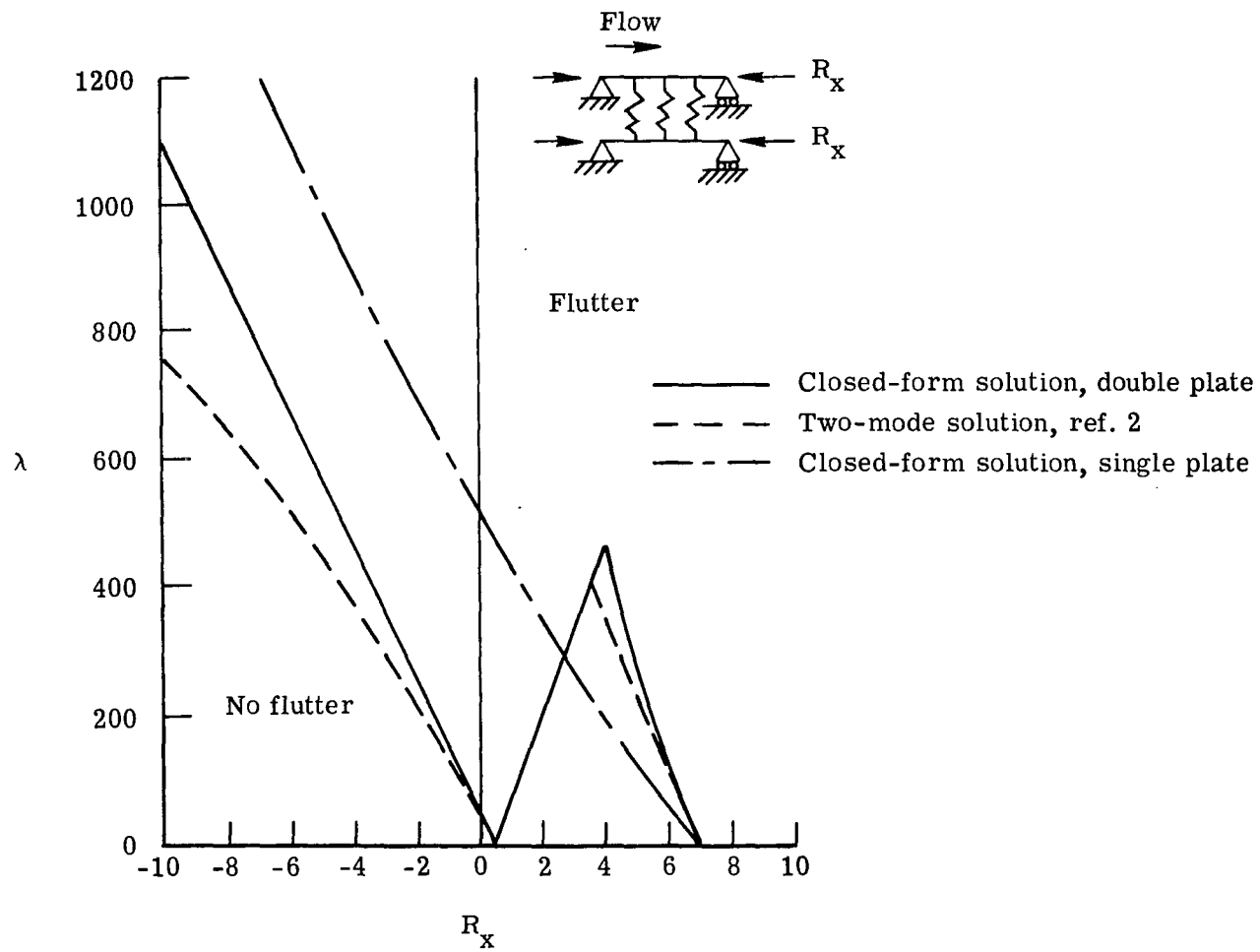Figure 3.- Vibration modes which coalesce for flutter of simply supported identical plates.   S = 10.

Figure 4.- Flutter boundaries for simply supported identical plates. $a/b = 4$; $S = 10$.

(a) S = 20.

Figure 5.- Closed-form and two-mode flutter boundaries for simply supported
identical plates. a/b = 1.

(b) S = 10.

Figure 5.- Concluded.
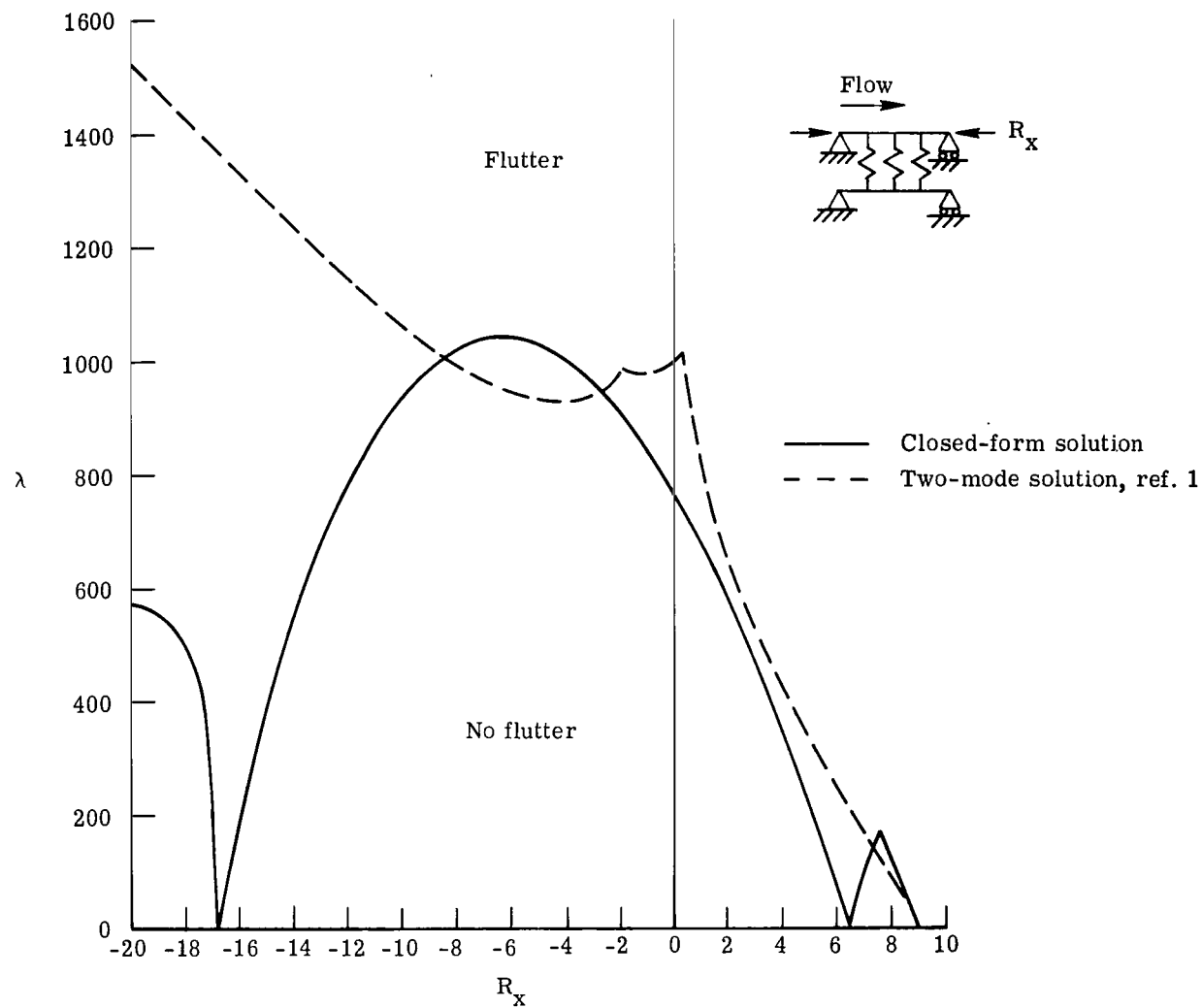
(a) Upper plate subjected to inplane loading.

Figure 6.- Closed-form and two-mode flutter boundaries with one plate subjected to inplane loading.   S = 20.
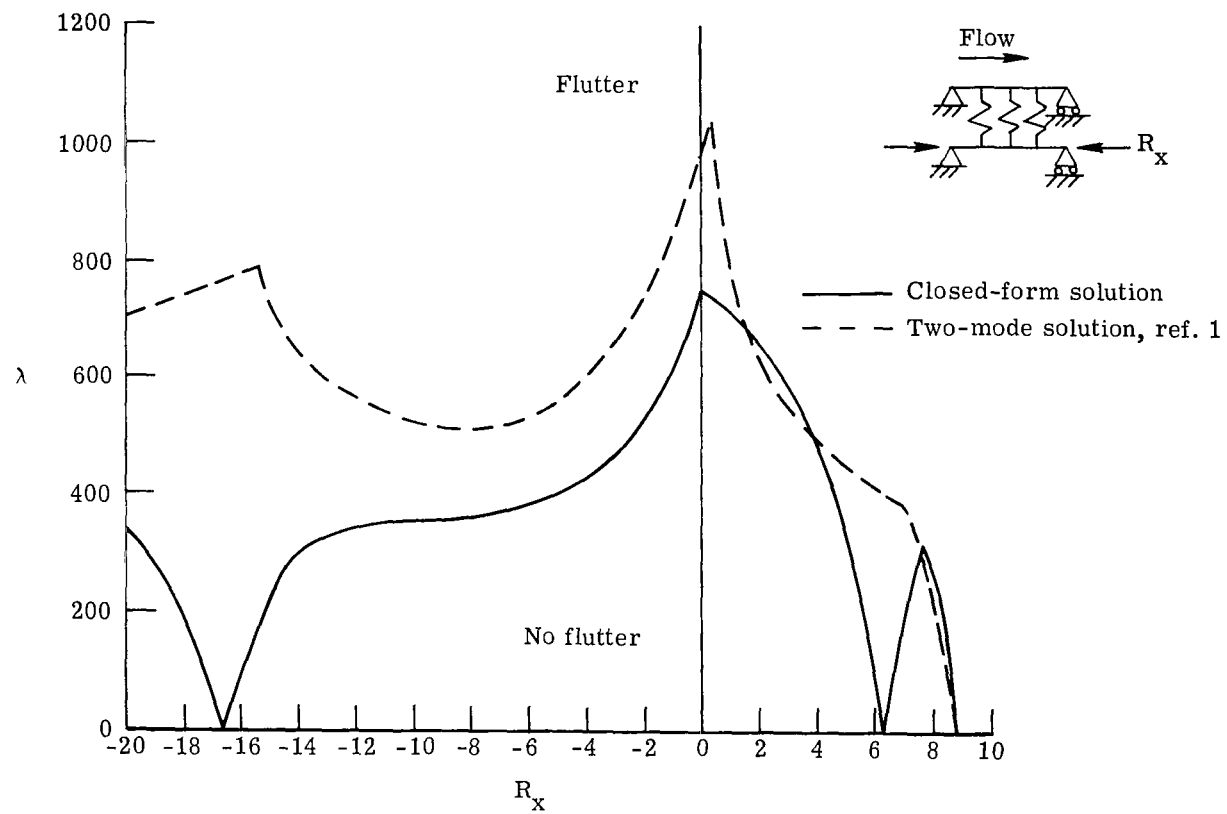
(b) Lower plate subjected to inplane loading.

Figure 6.- Concluded.
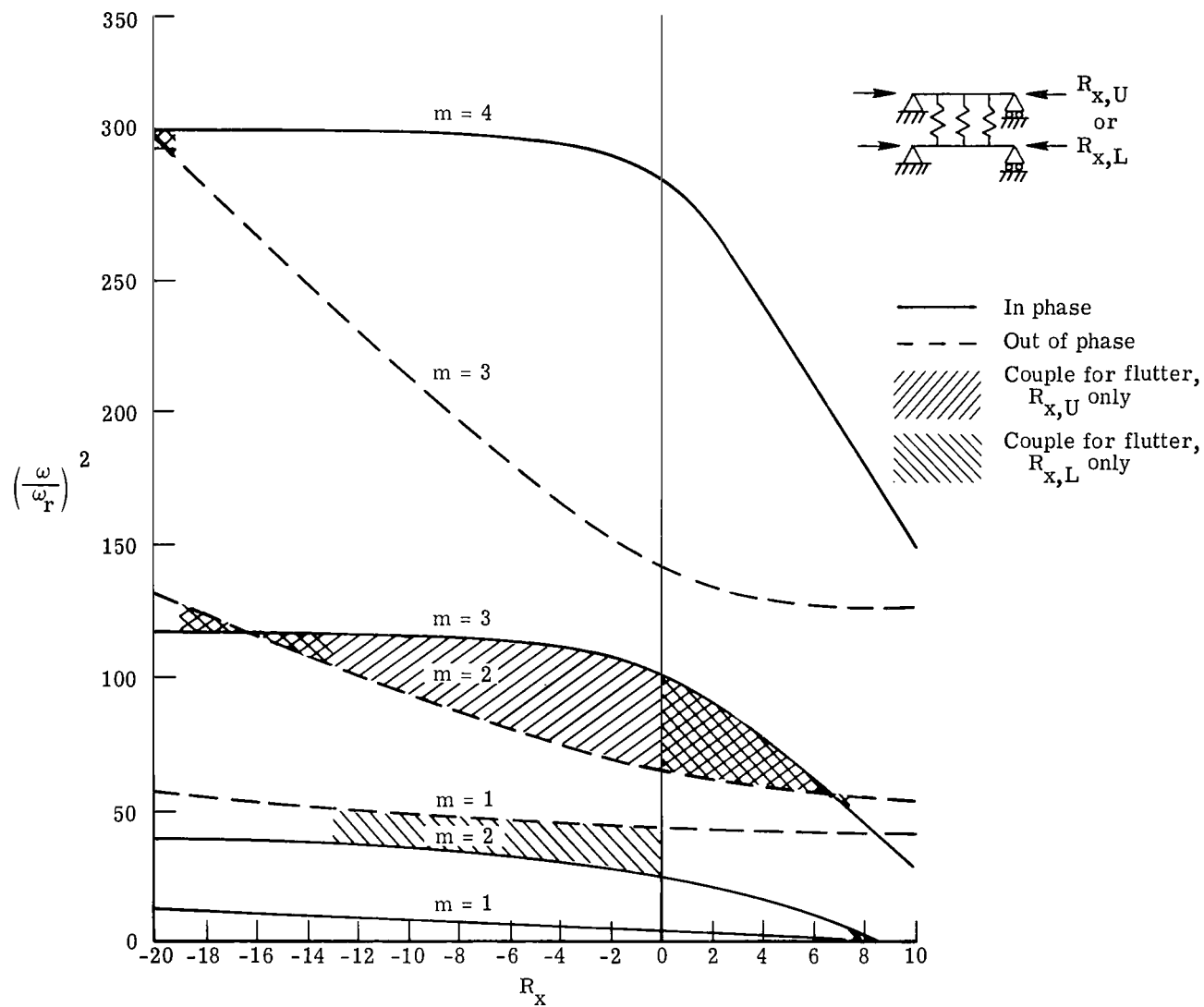
Figure 7.- Natural frequencies for elastically coupled, simply supported plates
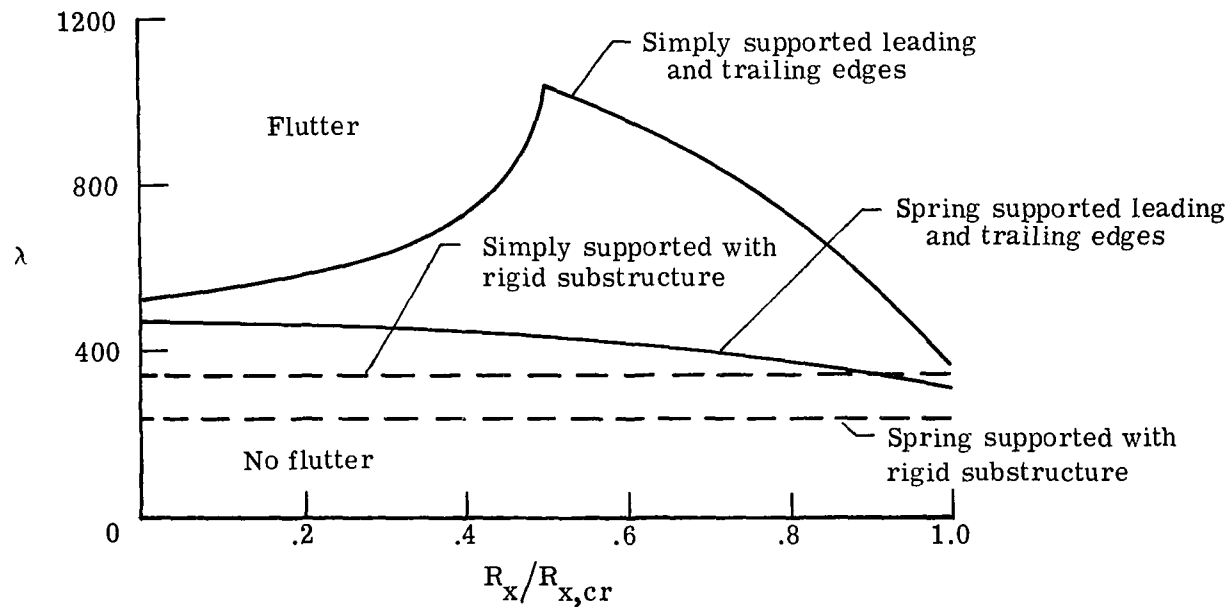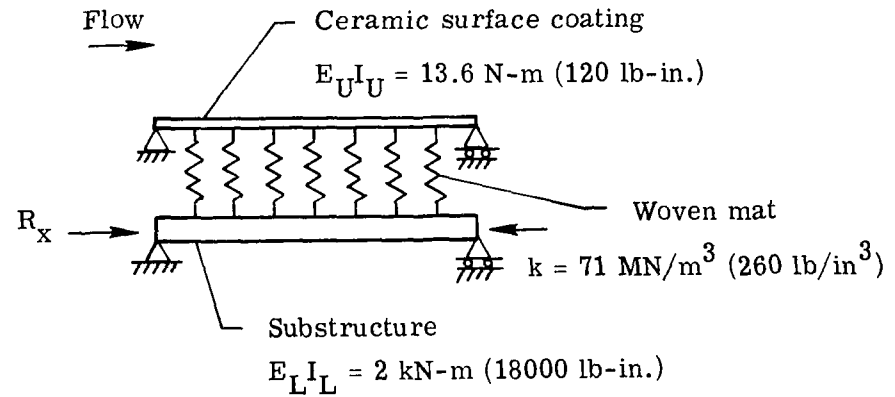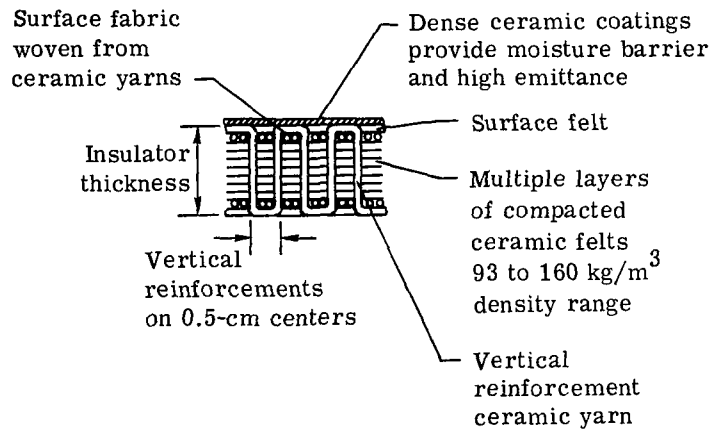with one plate subjected to inplane loading.   a/b = 1;   S = 20.

Schematic of woven mat

Surface fabric
woven from
ceramic yarns

Dense ceramic coatings
provide moisture barrier
and high emittance

Surface felt

Insulator
thickness

Multiple layers
of compacted
ceramic felts
93 to 160 kg/m^3
density range

Vertical
reinforcements
on 0.5-cm centers

Vertical
reinforcement
ceramic yarn

Flow

Ceramic surface coating

$E_U I_U$ = 13.6 N-m (120 lb-in.)

R_x

Woven mat

k = 71 MN/m^3 (260 lb/in^3)

Substructure

$E_L I_L$ = 2 kN-m (18000 lb-in.)

Flutter

Simply supported leading
and trailing edges

Spring supported leading
and trailing edges

Simply supported with
rigid substructure

Spring supported with
rigid substructure

No flutter

λ

$R_x / R_{x,cr}$
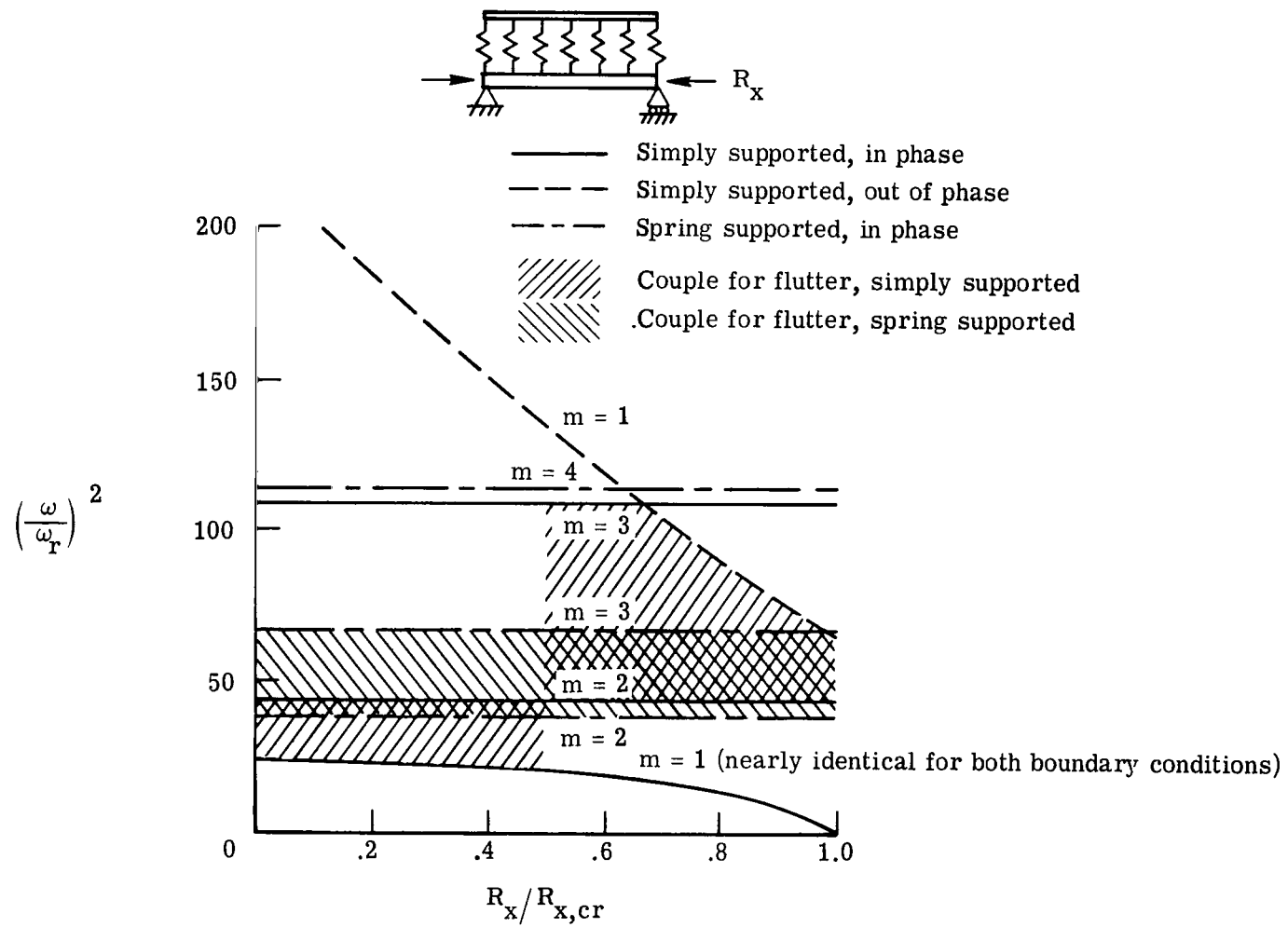
Figure 8.- Flutter boundaries for proposed TPS.
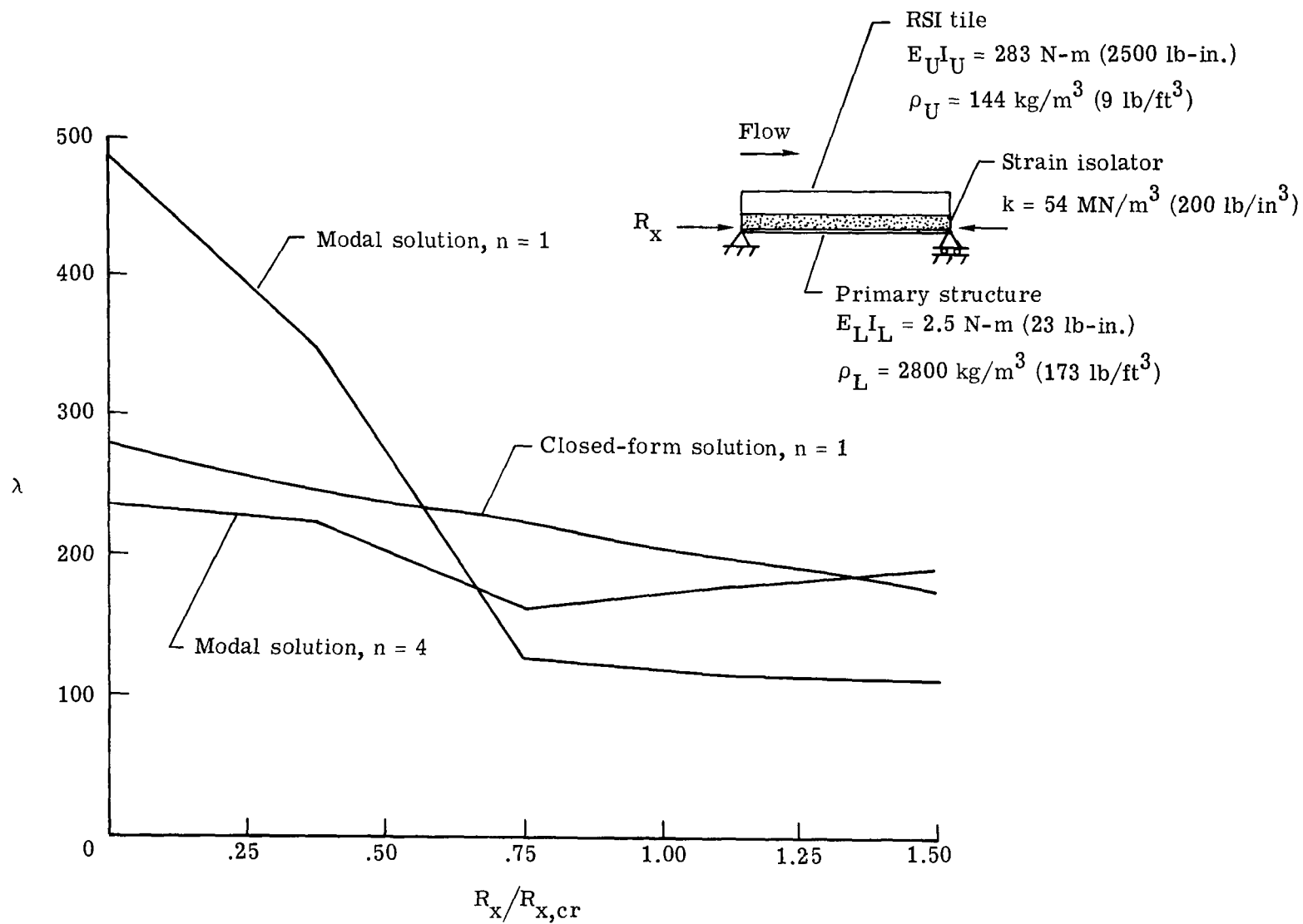
Figure 9.- Natural frequencies for proposed TPS.

Figure 10.- Closed-form and modal flutter boundaries for RSI panels. $R_{x,cr}$ is for primary structure only.
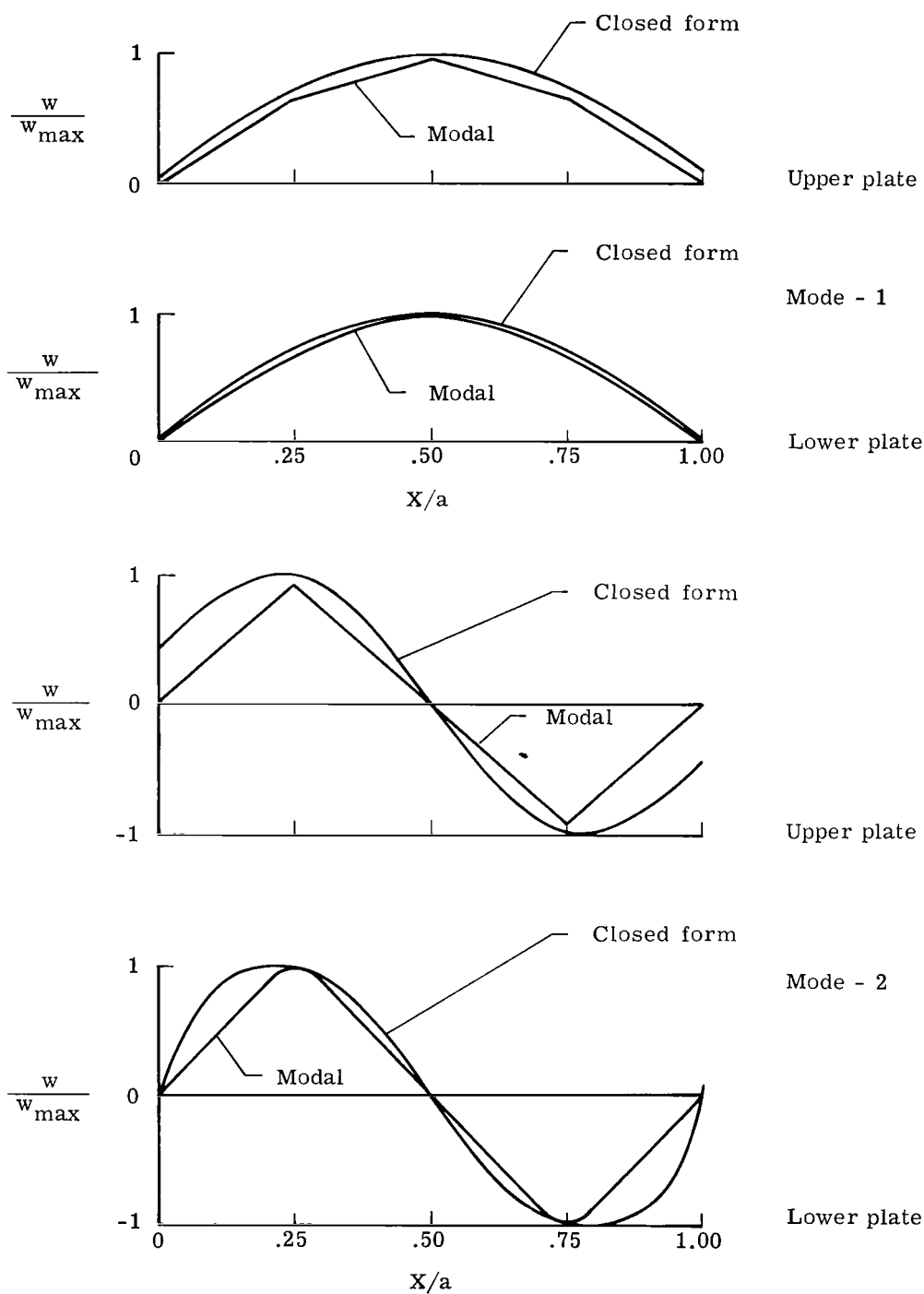
Figure 11.- Mode shapes from n = 1 closed-form and
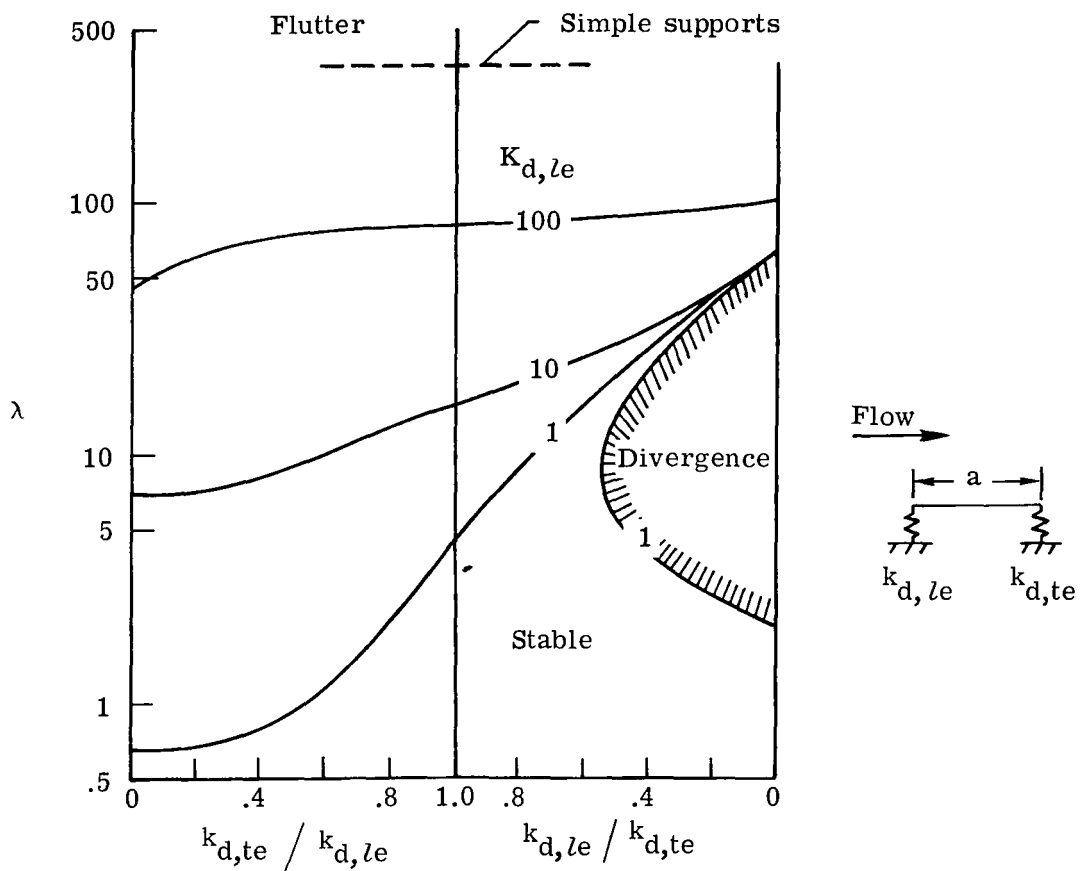n = 4 modal analyses of RSI panels.

Figure 12.- Effects of unequal edge spring supports on flutter of single plates.

118 001 C1 U D 751204 S00903DS
DEPT OF THE AIR FORCE
AF WEAPCNS LABORATOFY
ATTN: TECHNICAL LIBRAFY (SUL)
KIRTLAND AFB NM 87117

"*The aeronautical and space activities of the United States shall be conducted so as to contribute . . . to the expansion of human knowledge of phenomena in the atmosphere and space. The Administration shall provide for the widest practicable and appropriate dissemination of information concerning its activities and the results thereof.*"
—NATIONAL AERONAUTICS AND SPACE ACT OF 1958

NASA SCIENTIFIC AND TECHNICAL PUBLICATIONS

TECHNICAL REPORTS: Scientific and technical information considered important, complete, and a lasting contribution to existing knowledge.

TECHNICAL NOTES: Information less broad in scope but nevertheless of importance as a contribution to existing knowledge.

TECHNICAL MEMORANDUMS: Information receiving limited distribution because of preliminary data, security classification, or other reasons. Also includes conference proceedings with either limited or unlimited distribution.

CONTRACTOR REPORTS: Scientific and technical information generated under a NASA contract or grant and considered an important contribution to existing knowledge.

TECHNICAL TRANSLATIONS: Information published in a foreign language considered to merit NASA distribution in English.

SPECIAL PUBLICATIONS: Information derived from or of value to NASA activities. Publications include final reports of major projects, monographs, data compilations, handbooks, sourcebooks, and special bibliographies.

TECHNOLOGY UTILIZATION PUBLICATIONS: Information on technology used by NASA that may be of particular interest in commercial and other non-aerospace applications. Publications include Tech Briefs, Technology Utilization Reports and Technology Surveys.

Details on the availability of these publications may be obtained from:

SCIENTIFIC AND TECHNICAL INFORMATION OFFICE

NATIONAL AERONAUTICS AND SPACE ADMINISTRATION

Washington, D.C. 20546